ELSEVIER

Journal of Organometallic Chemistry 544 (1997) 257–276

Journal of Organometallic Chemistry

Nucleophilic and electrophilic reactions of C_5 *cyclo*-polyenes coordinated to the $[CpMoL_2]^{n+}$ fragment ($n = 1,2$; L = 1/2dppe, PMe_3, $P(OMe)_3$, CO)

Cristina G. de Azevedo [a], Maria J. Calhorda [b,c], M.A.A.F. de C.T. Carrondo [a,b], Alberto R. Dias [a], M. Teresa Duarte [a], Adelino M. Galvão [a], Carla A. Gamelas [b], Isabel S. Gonçalves [b], Fátima M. da Piedade [c], Carlos C. Romão [a,b,*]

[a] *Departamento de Engenharia Química, Instituto Superior Técnico, 1096 Lisboa Codex, Portugal*
[b] *Instituto de Tecnologia Química e Biológica, R. da Quinta Grande 6, 2780 Oeiras, Portugal*
[c] *Faculdade de Ciências da Universidade de Lisboa, 1700 Lisboa Codex, Portugal*

Received 12 May 1997

Abstract

Reaction of several nucleophiles (R^-) with the dications $[Cp_2MoL_2]^{2+}$ (L = CO, PMe_3, dppe) produces the cyclopentadiene complexes $[CpMo(\eta^4\text{-}C_5H_5R)L_2]^+$ (L = dppe, R = H, CH_3, CH_2CN, CH_2PPh_3, SMe; L = CO, R = H, CH_3, SPh, PMe_3; L = PMe_3, R = H). Excess nucleophiles only produces regio and stereospecific double addition to one Cp ring in the case of H^- forming $CpMo(\eta^3\text{-}C_5H_7)L_2$ (L = CO, PMe_3, dppe). $[CpMo(\eta^4\text{-}C_5H_6)L_2]^+$ reacts with $LiCuMe_2$ to give $CpMo(\eta^3\text{-}C_5H_6Me)L_2$ (L = dppe, CO) and $[Cp'Mo(\eta^4\text{-}C_5H_6)(CO)_2]^+$ reacts with NaSPh and PMe_3 to give $Cp'Mo(\eta^3\text{-}C_5H_6SPh)(CO)_2$ (Cp' = Cp, indenyl) and $[CpMo(\eta^3\text{-}C_5H_6PMe_3)(CO)_2]BF_4$ respectively. The structure of the exclusively formed conformers *endo*-$[CpMo(\eta^4\text{-}C_5H_6)(dppe)]PF_6$ and *endo*-$CpMo(\eta^3\text{-}C_5H_7)$(dppe) was determined by NMR and X-ray crystallography and analyzed by EHMO calculations. The reverse H^- abstractions from $[CpMo(\eta^4\text{-}C_5H_6)L_2]^+$ and $CpMo(\eta^3\text{-}C_5H_7)L_2$ with Ph_3C^+ are specific in all cases except for $CpMo(\eta^3\text{-}C_5H_7)$(dppe) which gives oxidative decomposition to $[Cp_2Mo(dppe)]^{2+}$ and $[CpMo(dppe)_2]^{2+}$. All the complexes $[CpMo(\eta^4\text{-}C_5H_5R)L_2]^+$ and $CpMo(\eta^3\text{-}C_5H_7)L_2$ (L = CO, PMe_3, dppe) as well as their C6 ring congeners $[CpMo(\eta^4\text{-}C_6H_8)(CO)_2]^+$ and $CpMo(\eta^3\text{-}C_6H_9)(CO)_2$ have irreversible cyclovoltammograms. Nucleophilic attacks of Me_3NO/NCMe and PMe_3 to $[CpMo(\eta^4\text{-}C_6H_8)(CO)_2]^+$ gave $[CpMo(\eta^4\text{-}C_6H_8)(NCMe)_2]BF_4$ and $[CpMo(\eta^3\text{-}C_6H_8PMe_3)(CO)_2]BF_4$ respectively. Both were crystallographically characterized. © 1997 Elsevier Science S.A.

1. Introduction

The fragment $[CpMo(CO)_2]^+$ is very useful in promoting and assisting a number of *regio* and *stereo* controlled transformations of coordinated unsaturated hydrocarbons, namely dienes and allyls. The synthetic sequence depicted in Scheme 1 exemplifies a protocol for 1,3-disubstitution of cyclohexadiene [1–5]. Similar examples exist for C_7 rings [6]. These are simply understood on the basis of the Davies–Green–Mingos rules governing kinetically controlled nucleophilic addition to the hydrocarbon ligands of 18-electron organometallic complexes [7–9].

In principle, these applications may be extended to C_5 rings potentially useful for the synthesis of cyclopentanoid terpenes and the expanding chemistry of substituted and functionalized cyclopentadienyl organometallic complexes [10–13]. Indeed, earlier work has established double sequential nucleophilic H^- addition to one of the Cp rings of $[Cp_2Mo(dppe)]^{2+}$ to give *regio* and *stereo* controlled 1,2 addition to the C_5 ring as in Scheme 2 (L_2 = dppe, dppm) [14].

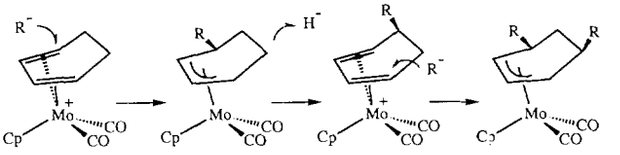

Scheme 1.

* Corresponding author. Tel.: +351 1 4418407; fax: +351 1 4411277; e-mail: ccr@itqb.unl.pt

0022-328X/97/$17.00
PII S0022-328X(97)00331-8

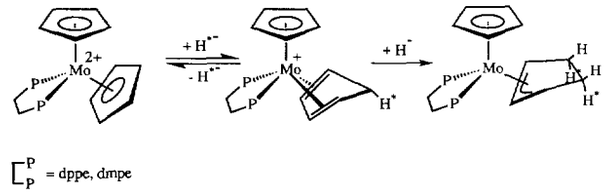

Scheme 2.

However, the preliminary attempts to extend these additions to the more useful carbon nucleophiles were unsuccessful although the formation of $CpMo(\eta^3\text{-}C_5H_5Cp_2)(CO)_2$, or its W analogue, from CpNa and $CpMo(CO)_2Cl_3$ may be regarded as a related result albeit mechanistically unclear [15]. More recently, we developed some chemistry of cyclopentadienes coordinated to the fragment $[CpMo(CO)_2]^+$ [16–18]. This has prompted us to reexamine the possibility of studying the 1,2-difunctionalization of C_5 rings according to the reaction steps of Scheme 2, i.e. double, sequential, nucleophilic addition to a molybdenocene dication, $[Cp_2MoL_2]^{2+}$. Although the C_6 and C_7 ring functionalizations mentioned above use CO as a spectator ligand [1–6], the L_2 spectator ligands may be easily changed in our system therefore providing further handles for stereo and/or electronic control of the reactivity of the cyclopentadiene or cyclopentadienyl rings towards nucleophilic addition. (L_2 = dppe, dppm, $(PMe_3)_2$, $\{P(OMe)_3\}_2$, $(CO)_2$, $MeSCH_2CH_2SMe$, $H_2NCH_2CH_2NH_2$).

In contrast to the well established predictive rules governing nucleophilic addition, no similar ones exist that predict the outcome of electrophilic reactions as the ones involved in the second step of Scheme 1, the reverse reaction of Scheme 2, and many of those usually employed for the final decomplexation of the functionalized C_5 ring (e.g. protonation, oxidation with I_2, Ce^{4+}).

In this paper we report the results of the compared structural, reactivity and electrochemistry studies on $[CpMo(cyclopentadiene)L_2]^+$ and CpMo(cyclopentenyl)L_2 complexes (L_2 = dppe, dppm, $(PMe_3)_2$, $\{P(OMe)_3\}_2$, $(CO)_2$, $MeSCH_2CH_2SMe$, $H_2NCH_2CH_2NH_2$) including the attempted 1,2-difunctionalization of C_5 rings with the $[CpMoL_2]^+$ and $[Cp_2MoL_2]^{2+}$ fragments.

The crystal structures of $[CpMo(\eta^4\text{-}C_5H_6)(dppe)]PF_6$, $CpMo(\eta^3\text{-}C_5H_7)(dppe)$, $[CpMo(\eta^3\text{-}C_6H_8PMe_3)(CO)_2]BF_4$ and $[CpMo(\eta^4\text{-}C_6H_8)(NCMe)_2]BF_4$ are presented.

2. Results

2.1. Chemical studies

The following studies comprise three families of complexes, namely, the dicationic molybdenocenes $[Cp_2MoL_2]^{2+}$, the monocationic diene derivatives $[CpMo(\eta^4\text{-}C_5H_5R)L_2]^+$ and the neutral allylic complexes $CpMo(\eta^3\text{-}C_5H_5R_2)L_2$.

The five dications selected were $[Cp_2Mo(dppe)][PF_6]_2$ (**1**) [14], $[Cp_2Mo(PMe_3)_2][PF_6]_2$ (**2**) [19], $[Cp_2Mo(CO)_2][BF_4]_2$ (**3**) [16–18], $[Cp_2Mo\{P(OMe)_3\}_2][BF_4]_2$ (**4**), $[Cp_2Mo(en)][BF_4]_2$ (**5**) [20], $[Cp_2Mo(dth)][BF_4]_2$ (**6**) [21] (en = ethylenediamine; dth = dithiohexane = $MeSCH_2CH_2SMe$).

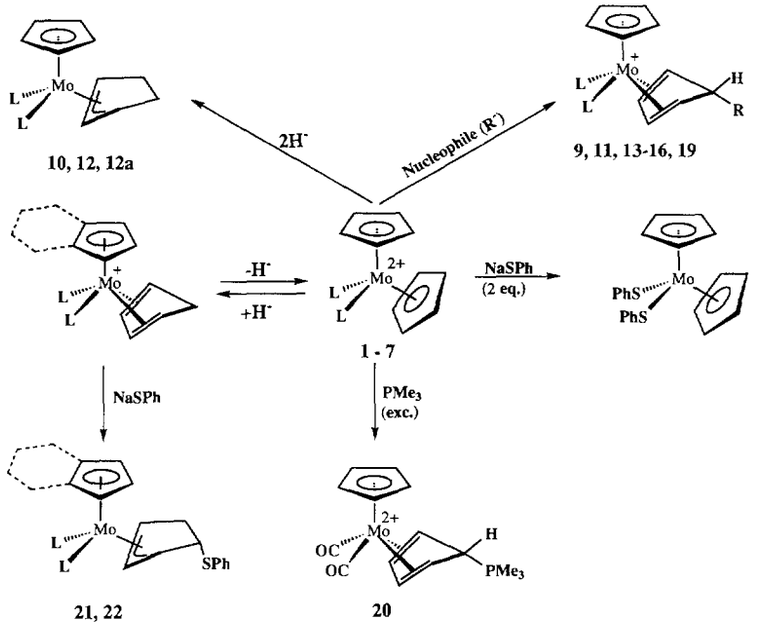

Scheme 3.

All but **4** are known species which have been previously reported. Conveniently improved preparations of **1** and **2** were developed by reacting Cp_2MoI_2, $TlPF_6$ and excess phosphine in NCMe or Me_2CO, respectively. When the reaction with PMe_3 is carried out in NCMe, the dication $[Cp_2Mo(NCMe)(PMe_3)][PF_6]_2$ (**7**) is formed in 85% yield.

1 and **4** are also obtained by reaction of **3** with dppe (80% yield) or $P(OMe)_3$ (70% yield) under irradiation and reflux but **2** is not available with this method since PMe_3 adds to the Cp ring (see **20** below).

The reaction of $Cp_2Mo(H)I$ with PMe_3 in the presence of $TlBF_4$, in Me_2CO, gives **2** in 42% yield but in NCMe $[Cp_2Mo(H)PMe_3]I$ (**8**) is also formed along with **2** in a proportion of 70:30. For the sake of comparison it should be noted that the corresponding reaction with dppe gives mainly $[CpMo(\eta^4\text{-}C_5H_6)(dppe)]^+$ (**9**) and only a very small amount of **1** [22].

A general summary of the reactions of these cations with nucleophiles R^- (R = H, alkyl, SR, PMe_3) is presented in Scheme 3.

The sequential hydride addition depicted in Scheme 2 takes place readily with H^- adding to the external face of the Cp ring. This stereochemistry was established earlier on the basis of labelling studies: D^- addition to **1** gave $[CpMo(\eta^4\text{-}C_5H_5D)(dppe)]^+$ (**9**–D) where the low frequency ν(C–H) vibration typical of the *exo* C–H bond of the methylene group of C_5H_6 is absent [14]. The VT ^{1}H NMR spectrum of $[CpMo(\eta^4\text{-}C_5H_6)(dppe)]PF_6$ (**9**) shows that the compound has a non-fluxional structure and that only one of the two possible conformational isomers **a** or **b** (R = H) is formed. This has now been assigned as the *endo* conformation, **a** (R = H) by means of a detailed analysis of the ^{1}H NMR spectrum using the method introduced by Davies and co-workers [23].

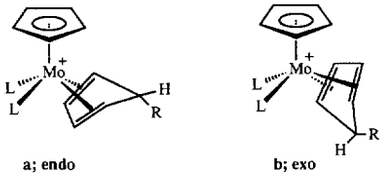

The method is based on the fact that long range coupling of the P atoms of dppe with H_{exo}, occurring over four bonds in a "W" arrangement, is only possible in the *endo* conformer **a**. Accordingly, the resonance of H_{exo} at δ 3.58 ppm (**a**, R = H_{exo}) is left as a triplet ($^4J_{P-H}$ = 9.7 Hz) upon selective decoupling of the geminal H_{endo} (δ 2.57 ppm). As described for other cyclopentadiene complexes this long range coupling of H_{exo} with P is equal to the coupling between H_{endo} and the other diene protons (J_{H-H} = 9.7 Hz) but larger than the coupling between H_{exo} and the diene protons which is < 2 Hz [23].

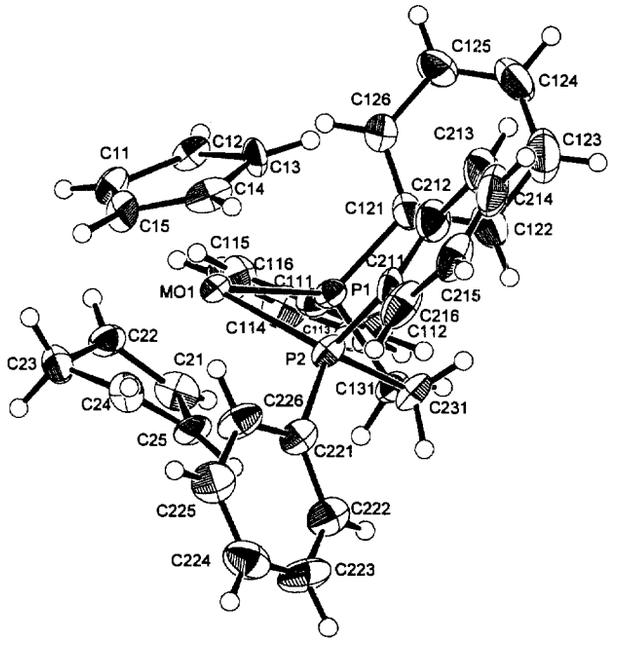

Fig. 1. ORTEP drawing of the complex $[CpMo(\eta^4\text{-}C_5H_6)(dppe)]^+$ (9^+) with the atom numbering scheme.

A crystal structure determination of $[CpMo(\eta^4\text{-}C_5H_6)(dppe)]PF_6 \cdot CH_2Cl_2$ (**9**) confirmed this structural assignment (see below, Fig. 1).

Hydride addition to *endo*-$[CpMo(\eta^4\text{-}C_5H_6)(dppe)]PF_6$ (**9**) [14], gives the structurally rigid isomer *endo*-$CpMo(\eta^3\text{-}C_5H_7)(dppe)$ (**10**). This was ascertained by means of a crystal structure determination (see below, Fig. 2) since the ^{1}H NMR spectrum is uninformative due to superposition of η^3-C_5H_7 and dppe resonances.

Similar hydride additions also take place readily with the dications $[Cp_2Mo(PMe_3)_2][PF_6]_2$ (**2**) and $[Cp_2Mo(CO)_2][BF_4]_2$ (**3**). The former reacts with excess $NaBH_4$ to give the cyclopentadiene complex $[CpMo(\eta^4\text{-}C_5H_6)(PMe_3)_2]PF_6$ (**11**). The VT ^{1}H NMR spectrum of **11** remains sharp and unchanged between −70°C and room temperature in agreement with the presence of only one isomer in solution. The arguments given below in Section 2.4 led to the assumption that this was, again, the *endo* isomer, **a** (R = H; L = PMe_3) as in the case of **9**. The chemical shifts of the methylene protons of the C_5H_6 ring are very similar to those observed for **9** and, therefore, we assigned the H_{exo} as the higher field resonance at δ 2.60 ppm and H_{endo} as the lower field resonance at δ 4.04 ppm. Also as expected, the Cp resonance appears as a triplet due to coupling to both PMe_3 ligands $^3J(^{31}P-^1H$ = 1.6 Hz). However, quite unexpectedly, no coupling between H_{exo} and the PMe_3 ligands was observed as predicted for the *endo* isomer where the W arrangement between the P atoms and H_{exo} is verified. This situation might suggest the *endo* conformation **b** for the actual isomer **11**. Since

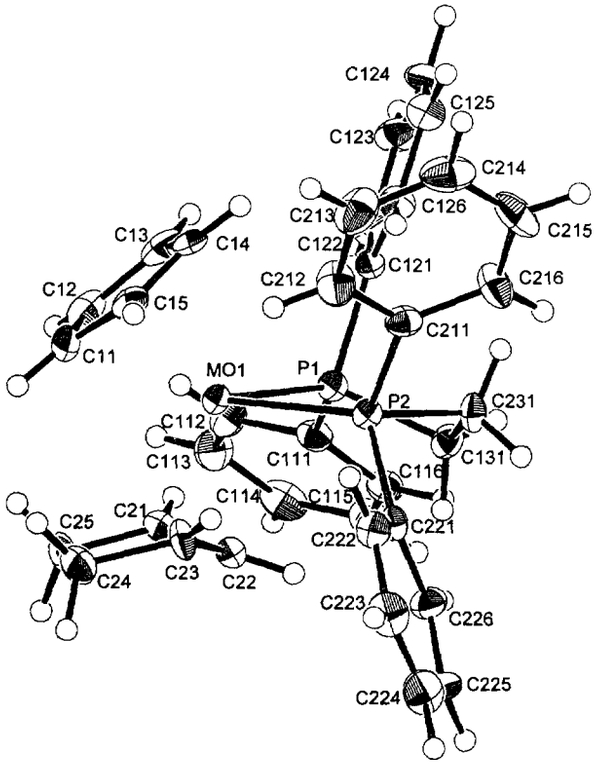

Fig. 2. ORTEP drawing of the complex CpMo(η^3-C_5H_7)(dppe) (**10**) with the atom numbering scheme.

a crystal structure has shown that **11** is, indeed, the *endo* isomer **a** [24], we must conclude that the coupling criterium must be used with due care. As a matter of fact, some of the coupling values given in the literature are rather small and may eventually vanish due to rather sensitive electronic and/or steric factors [23].

Addition of H^- to the [CpMo(η^4-C_5H_6)(PMe_3)$_2$]PF_6 (**11**) requires the use of $LiAlH_4$ and gives CpMo(η^3-C_5H_7)(PMe_3)$_2$ (**12**). This product is not fluxional and is considered to have the *endo* conformation which originates from the external H^- addition to the terminal C atom of the diene in **11**, as shown in Scheme 4. Selective irradiation of the ^{1}H NMR peaks allowed detailed assignment of all the resonances. The *meso* allylic proton (δ 2.59 ppm) is coupled to both P atoms: $^3J(^{31}P-^1H_7) = 10.4$ Hz).

Sequential double hydride addition to [Cp_2Mo-$(CO)_2$][BF_4]$_2$ (**3**), using $LiAlH_4$ in THF, forms the known CpMo(η^3-C_5H_7)$(CO)_2$ [25] whereas reaction of **3** with $NaBH_4$ in Me_2CO, gives [Cp_2MoH(CO)]BF_4

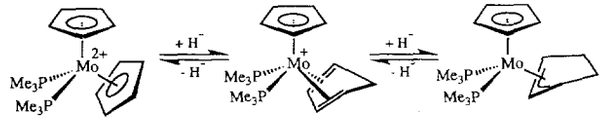

Scheme 4.

(ligand substitution). Reaction of [Cp_2Mo(en)]I_2 with $NaBH_4$ in 1,2-dimethoxyethane suspension gives a cerise complex identified as [CpMo(η^4-C_5H_6)(en)]PF_6 (**13**) after counter-ion metathesis. This identification is based on the presence of the *exo* C–H stretching vibration at 2775 cm^{-1} and elemental analysis. The ^{1}H NMR spectrum was not fully interpreted due to the complexity inherent to the presence of isomers and broad N*H* resonances. No traces of any neutral complex corresponding to CpMo(η^3-C_5H_7)(en) was detected in any of the several attempts. No tractable product is formed upon reaction of the dithiohexane derivative [Cp_2Mo(dth)][BF_4]$_2$ with BH_4^- or $LiAlH_4$.

The first attempts to add carbon nucleophiles to the dication [Cp_2Mo(dppe)][PF_6]$_2$ (**1**) using MeMgBr, LiPh, LiMe led to untractable mixtures. However, the softer alkylating agent $LiCuMe_2$ reacts with **1** to give the monomethylated adduct [CpMo(η^4-C_5H_5Me)(dppe)]PF_6 (**14**). Similarly, the stabilized carbanion $LiCH_2CN$ and the ylid CH_2PPh_3 add to **1** giving [CpMo(η^4-$C_5H_5CH_2CN$)dppe]PF_6 (**15**) and [CpMo(η^4-$C_5H_5CH_2PPh_3$)(dppe)]PF_6 (**16**), respectively. All these reactions are done adding the dication to a cooled solution of the carbon nucleophile in order to minimize side reactions. The absence of the low frequency ν(C–H_{exo}) vibration in the IR spectra is in agreement with the expected addition of the nucleophile R^- to the external face of the Cp ring as in **a** or **b**. The ^{1}H NMR spectra of [CpMo(η^4-C_5H_5Me)(dppe)]PF_6 (**14**), [CpMo(η^4-$C_5H_5CH_2CN$)(dppe)]PF_6 (**15**) and [CpMo(η^4-$C_5H_5CH_2PPh_3$)(dppe)]PF_6 (**16**) all show only one non-fluxional isomer. Although the resonance assignment is straightforward, the data do not allow a clear telling about the isomer stereochemistry although the *endo* conformation **a** (R = Me, CH_2CN, CH_2PPh_3) is assumed on the basis of reactivity arguments (see Section 3).

Use of excess of the carbon nucleophile ($LiCuMe_2$ or $LiCH_2CN$) under several experimental conditions at or below room temperature failed to give a second addition. No reaction or decomposition to untractable products was observed. This decomposition was first attributed to the facile deprotonation of the cyclopentadiene cation [CpMo(η^4-C_5H_5R)(dppe)]$^+$ formed after the first R^- addition. However, this may not be the case because [CpMo(η^4-C_5H_6)(dppe)]$^+$ (**9**) resists deprotonation by NEt_3 (unlike its carbonyl analogue [CpMo(η^4-C_5H_6)$(CO)_2$]$^+$ which gives Cp(η^3-Cp)Mo$(CO)_2$) [18] but reacts with excess $LiCuMe_2$ to give CpMo(η^3-C_5H_6Me)(dppe) (**17**). Addition of enolates was briefly tested on **1** but no evidence of formation of the synthetically useful 1,2 double addition products was obtained.

Reaction of [Cp_2Mo$(CO)_2$][BF_4]$_2$ (**3**) with two equivalents of $LiCH_2CN$ does not lead to the desired CpMo(η^3-1,2-$(CH_2CN)_2C_5H_5$)$(CO)_2$. Instead,

$[Cp_2Mo(CO)H]BF_4$ was the only product isolated as the known $[Cp_2Mo(CO)Cl]BF_4$ (characterized by ^1H NMR and analysis). No product could be identified from the reaction of **3** or $[Cp_2Mo\{P(OMe)_3\}_2][BF_4]_2$ (**4**) with two equivalents or excess of $LiCuMe_2$. However, reaction of $[CpMo(\eta^4\text{-}C_5H_6)(CO)_2]BF_4$ [16–18], with a slight excess of $LiCuMe_2$ led to the expected addition at the diene ring with formation of the allylic complex $CpMo(\eta^3\text{-}C_5H_6Me)(CO)_2$ (**18**) in fair yield (60%).

Less basic strong nucleophiles, also add to the Cp and the cyclopentadiene rings but double sequential addition was never detected. NaSMe reacts with $[Cp_2Mo(dppe)][PF_6]_2$ (**1**) to give the monosubstituted diene complex $[CpMo(\eta^4\text{-}C_5H_5SMe)(dppe)]PF_6$ (**19**) even when excess thiolate was used. Addition to the external face of the diene is implied by the absence of the $C\text{–}H_{exo}$ vibration as in all other cases so far. The reaction with NaSPh is more complex. At −25°C in THF a very temperature and hydrolysis sensitive product is formed which is very similar to **19** (IR evidence) but which was not further characterized. Excess NaSPh under more forcing conditions (refluxing 1,2-dme for 4 h or longer time at room temperature) led to the well known bis-thiolate $Cp_2Mo(SPh)_2$ in 78% yield [26]. Only ligand substitution is observed for the reactions of $[Cp_2Mo(CO)_2][BF_4]_2$ (**3**) with NaSPh: with 1 equivalent, in CH_2Cl_2, $[Cp_2Mo(CO)(SPh)]BF_4$ (ν(CO) = 2041 cm^{-1}) is formed whereas 2 equivalents lead to $Cp_2Mo(SPh)_2$.

Instead of substituting CO, the neutral nucleophile PMe_3 readily adds to the external face of the cyclopentadienyl ligand of **3** to give $[CpMo(\eta^4\text{-}C_5H_5PMe_3)(CO)_2][BF_4]_2$ (**20**). Both isomers, **a** and **b** (L = CO; R = PMe_3) are observed at room temperature in the ^1H NMR spectrum.

These soft S and P nucleophiles also add to the cyclopentadiene complexes. PhS^- adds to the C_5H_6 ring of both $[CpMo(\eta^4\text{-}C_5H_6)(CO)_2]BF_4$ and $[IndMo(\eta^4\text{-}C_5H_6)(CO)_2]BF_4$ to give $Cp'Mo(\eta^3\text{-}C_5H_6SPh)(CO)_2$ [Cp′ = Cp (**21**), Ind (**22**)]. PMe_3 adds to the cyclopentadiene ring of $[CpMo(\eta^4\text{-}C_5H_6)(CO)_2]BF_4$ and to the cyclohexadiene ring of $[CpMo(\eta^4\text{-}C_6H_8)(CO)_2BF_4$ to give $[CpMo(\eta^3\text{-}C_5H_6PMe_3)(CO)_2]BF_4$ (**23**) and $[CpMo(\eta^3\text{-}C_6H_8PMe_3)(CO)_2]BF_4$ (**24**), respectively. $PHPh_2$ does not give any reaction. Both **23** and **24** resist deprotonation by NEt_3. The former reacts with Ph_3CBF_4 to regenerate $[CpMo(\eta^4\text{-}C_5H_6)(CO)_2]BF_4$. The X-ray crystal structure of **24** is depicted in Fig. 3.

Harder or more basic nucleophiles do not give isolable adducts. Reaction of $[Cp_2Mo(dppe)]^{2+}$ (**1**) with sodium methoxide gives an ill defined uncharacterized product but cyanide (KCN) did not react even under drastic reflux conditions. Reaction of $KPPh_2$ with **1** leads to decomposition and with $[CpMo(\eta^4\text{-}C_5H_6)(CO)_2]BF_4$ initial deprotonation is observed (the green colour suggestive of $Cp(\eta^3\text{-}Cp)Mo(CO)_2$ is immediately formed) also followed by decomposition.

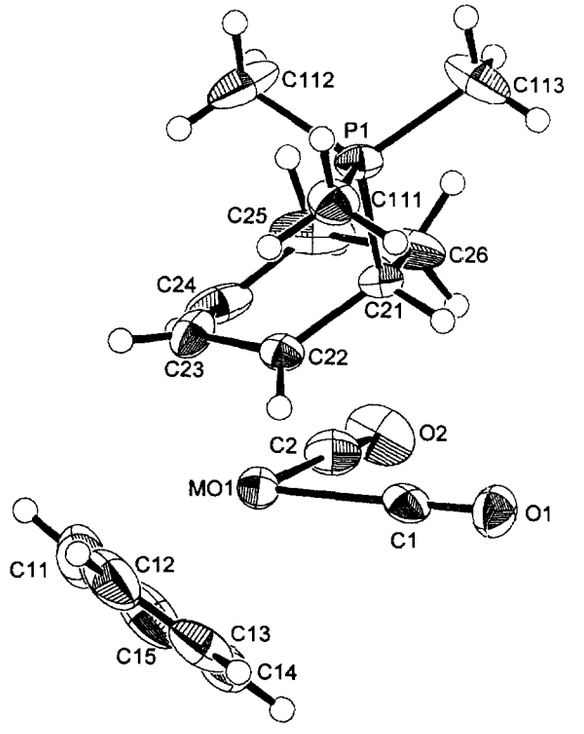

Fig. 3. ORTEP drawing of the complex $[CpMo(\eta^3\text{-}C_6H_8PMe_3)(CO)_2]^+$ (**24**$^+$) with the atom numbering scheme.

While attempting to circumvent the rather complex synthesis of the structurally characterized $[CpMo(\eta^4\text{-}C_6H_8)(dppe)]PF_6$ [27,28], $[CpMo(\eta^4\text{-}C_6H_8)(CO)_2]BF_4$ was treated with Me_3NO in the presence of excess dppe, in NCMe solvent. Instead of $[CpMo(\eta^4\text{-}C_6H_8)(dppe)]PF_6$ $[CpMo(\eta^4\text{-}C_6H_8)(NCMe)_2]BF_4$ (**25**) was obtained in 80% yield. The X-ray crystal structure of **25** is depicted in Fig. 4, but its chemistry was not studied further.

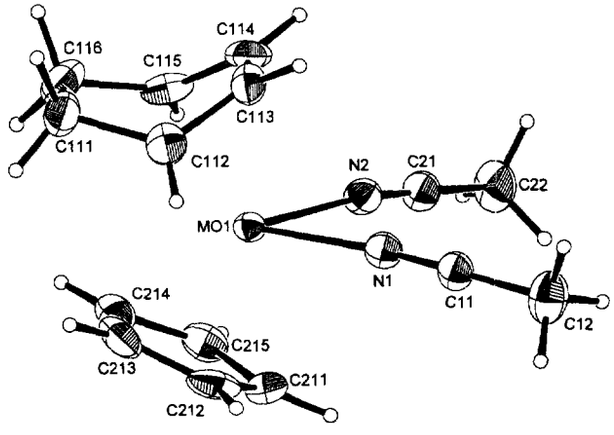

Fig. 4. ORTEP drawing of the complex $[CpMo(\eta^4\text{-}C_6H_8)(NCMe)_2]^+$ (**25**$^+$) with the atom numbering scheme.

In previous publications the H^- abstraction from coordinated C_5H_6 (Scheme 2, reverse of the first step) was extended to several cationic cyclopentadiene complexes $[Cp'Mo\text{-}(\eta^4\text{-}C_5H_6)L_2]^+$ (Cp' = Cp, Ind; L_2 = $(CO)_2$, dppe) [16–18]. We have now found that these abstractions may also be quantitatively performed by other oxidants, as Cl_2 or Br_2. Indeed, treatment of $[CpMo(\eta^4\text{-}C_5H_6)(dppe)]^+$ and $[Cp'Mo(\eta^4\text{-}C_5H_6)(CO)_2]^+$ with gaseous Cl_2, Br_2 or Br_3^-, in CH_2Cl_2, gives the corresponding dications $[Cp_2MoL_2]^{2+}$ and $[CpCp'MoL_2]^{2+}$ (Cp' = Cp, Ind; L_2 = $(CO)_2$, dppe) in quantitative yield. The ferricenium cation also reacts with $[CpMo(\eta^4\text{-}C_5H_6)(dppe)]^+$, in refluxing NCMe, to give the $[Cp_2Mo(dppe)]^{2+}$, albeit in only 45% isolated yield. In contrast, the corresponding cyclohexadiene and cycloheptatriene complexes $[CpMo(\eta^4\text{-}C_6H_8)(CO)_2]^+$ and $[CpMo(\eta^4\text{-}C_7H_8)(CO)_2]^+$ react neither with Cl_2 nor with Ph_3C^+ [18,29]. However, as reported in the literature and shown in Scheme 1, H^- abstraction with Ph_3C^+ from the cyclohexenyl complexes $CpMo(\eta^3\text{-}C_6H_8R)(CO)_2$ is totally reproducible and predictable [1]. In a similar vein, Ph_3C^+ reacts with $CpMo(\eta^3\text{-}C_5H_7)(CO)_2$ and $CpMo(\eta^3\text{-}C_5H_7)(PMe_3)_2$ to give $[CpMo(\eta^4\text{-}C_5H_6)L_2]^+$ which reacts with a second equivalent of Ph_3CBF_4, to give the dication $[Cp_2MoL_2]^{2+}$ (L = CO, PMe_3) as seen in Scheme 4 for the case of L = PMe_3.

The reaction also proceeds to the same final result without isolation of the intermediate $[CpMo(\eta^4\text{-}C_5H_6)L_2]^+$. Surprisingly, the reaction of the analogue $CpMo(\eta^3\text{-}C_5H_7)(dppe)$ with 1 equivalent of Ph_3CBF_4, in CH_2Cl_2 or THF, does not give $[CpMo(\eta^4\text{-}C_5H_6)(dppe)]BF_4$. Instead, a mixture of dications, namely the expected $[Cp_2Mo(dppe)][BF_4]_2$ (30%) and the known paramagnetic $[CpMo(dppe)_2][BF_4]_2$ (60%) is isolated [27,30]. The reaction of $CpMo(\eta^3\text{-}C_5H_7)(dppe)$ with $FcPF_6$ is totally irreproducible, giving a variety of unidentified paramagnetic species as judged from ESR spectra.

2.2. Electrochemical studies

The cyclic voltammograms of the cyclopentadienyl, cyclopentadiene and cyclopentenyl complexes, $[CpMo(dppe)_2]^{2+}$, $[Cp_2Mo(dppe)]^{2+}$, $[CpMo(\eta^4\text{-}C_5H_6)L_2]^+$ and $CpMo(\eta^3\text{-}C_5H_7)L_2$ (L_2 = $(CO)_2$, $(PMe_3)_2$, dppe) and some related complexes were studied in both CH_2Cl_2 and NCMe solvents as summarized in Table 1. Only minor variations of the peak potentials were registered indicating that no solvent dependent processes are present.

The cyclic voltammograms of both $[CpMo(\eta^4\text{-}C_5H_6)(CO)_2]^+$ and $[CpMo(\eta^4\text{-}C_6H_8)(CO)_2]^+$ do not show oxidation waves but only a totally irreversible reduction with a small cathodic response in the latter case. In contrast, the cyclic voltammograms of $[CpMo(\eta^4\text{-}C_5H_6)dppe]^+$ and $[CpMo(\eta^4\text{-}C_5H_6)(PMe_3)_2]^+$ present only irreversible oxidation waves.

The parent allylic complex $CpMo(\eta^3\text{-}C_3H_5)(CO)_2$ undergoes a reversible oxidation but its cyclopentenyl and the cyclohexenyl analogues, $CpMo(\eta^3\text{-}$

Table 1
Cyclovoltammetric data

Complex	E_{pa} (V)		E_{pc} (V)	Comment
$[CpMo(\eta^4\text{-}C_5H_6)(dppe)]BF_4$	$E_{pa1} = 0.70$	$E_{pa1} = 0.73$	–	all irreversible
	$E_{pa2} = 0.88$	$E_{pa2} = 0.91$	–	
	$E_{pa3} = 1.25$	$E_{pa3} = 1.25$	–	
	(NCMe)	(CH_2Cl_2)	–	
$[CpMo(\eta^4\text{-}C_5H_6)(CO)_2]BF_4$	−0.76		–	irreversible
	–		−0.95	
$[CpMo(\eta^4\text{-}C_6H_8)(CO)_2]BF_4$	−0.70		–	irreversible
	–		−1.07	
$[CpMo(\eta^4\text{-}C_5H_6)(PMe_3)_2]BF_4$	0.50		–	irreversible
	–		−1.02	
$CpMo(\eta^3\text{-}C_5H_7)(PMe_3)_2$	−0.60		−0.66	irreversible
	0.48		–	
$CpMo(\eta^3\text{-}C_3H_5)(CO)_2$	0.60		0.55	reversible
$CpMo(\eta^3\text{-}C_5H_7)(CO)_2$	0.69		–	irreversible
$CpMo(\eta^3\text{-}C_5H_7)(dppe)$	0.67 [a]		–	irreversible
$CpMo(\eta^3\text{-}C_6H_9)(CO)_2$	0.64		–	irreversible
$[Cp_2Mo(dppe)]^{2+}$	0.43		–	all irreversible
	0.78		–	
	1.28		–	
$[CpMo(dppe)_2]^{2+}$	1.28		–	irreversible
Ph_3CBF_4	–		−0.84	irreversible

E_{pa} = anodic sweep (peak potentials in V).
E_{pc} = cathodic sweep (peak potentials in V).
All the cyclic voltammograms in NCMe except [a] in CH_2Cl_2.

$C_5H_7)(CO)_2$, $CpMo(\eta^3\text{-}C_5H_7)(PMe_3)_2$, $CpMo(\eta^3\text{-}C_5H_7)$(dppe), $CpMo(\eta^3\text{-}C_6H_9)(CO)_2$, all present irreversible oxidation waves in NCMe. The value given for complex $CpMo(\eta^3\text{-}C_5H_7)$(dppe) should be regarded with some care as the voltammograms are rather difficult to reproduce by unknown reasons.

Both complexes $[CpMo(\eta^4\text{-}C_5H_6)(dppe)]^+$ and $[Cp_2Mo(dppe)]^{2+}$ present an oxidation wave at 1.28 V. The latter wave may be assigned to the oxidation of the Mo(III) dication $[CpMo(dppe)_2]^{2+}$ since it is the only wave registered in the cyclic voltammogram of this complex.

2.3. Crystallographic studies

2.3.1. Crystal structure of $[CpMo(\eta^4\text{-}C_5H_6)(dppe)]PF_6 \cdot CH_2Cl_2$ (9)

The structure of complex $\mathbf{9}^+$, shown in Fig. 1, can be regarded as another example of the family of $CpMo(\eta^4$-diene) derivatives with the *endo* conformation **a**. Selected bond lengths and angles for **9** are given in Table 2.

In the η^4-cyclopentadiene ring (CpH) the four atoms of the butadiene residue, C(21)C(22)C(24)C(25), are planar (max. dev. 0.001 Å for all carbon atoms), the fifth carbon atom C(23) is 0.517 Å away and the Mo atom is 2.013(9) Å away from that plane. The C–C bond distances are typical of a butadiene. The angle between the planes defined by the butadiene atoms and C(22)C(23)C(24), the fold angle, is 31°. The Cp and CpH rings have a staggered conformation, and the angle between the normals to the $\eta^5\text{-}C_5H_5$ and butadiene planes is 127.32(5)°, a smaller value than that reported by Prout [31] in the related complex $(\eta^5\text{-}C_5H_5)(\eta^4\text{-}1\text{-endo-}C_2H_5C_5H_5)MoP(C_2H_5)_3Cl$, viz. 131.2°, where steric interactions between the rings are present. The Mo–P distances of 2.471(2) and 2.479(2) Å in **9** are shorter than those in $[CpMo(\eta^4\text{-}C_6H_8)(dppe)][PF_6] \cdot SO_4$ (Mo–P are 2.500 and 2.492 Å) but the angles P–Mo–P (78.16(8)° and 77.8(1)°, respectively) are comparable [28]. The plane containing the normals is almost perpendicular (92.3°) to the plane containing the two Mo–P bonds.

While in the parent $[Cp_2MoLL']$ compounds the

Table 2
Selected bond lengths (Å) and angles (deg) for the complexes **9**, **10**, **24** and **25**

9		**10**		**24**		**25**	
Mo(1)–P(1)	2.471(2)	Mo(1)–P(1)	2.421(2)	Mo(1)–C(1)	1.922(10)	Mo(1)–N(1)	2.143(5)
P(1)–C(111)	1.819(9)	P(1)–C(131)	1.839(6)	P(1)–C(111)	1.767(11)	Mo(1)–C(213)	2.326(7)
P(1)–C(131)	1.847(8)	P(1)–C(111)	1.844(6)	P(1)–C(113)	1.789(10)	C(11)–C(12)	1.450(9)
P(2)–C(211)	1.855(9)	P(2)–C(231)	1.864(6)	C(1)–O(1)	1.156(11)	C(21)–C(22)	1.448(10)
P(2)–C(231)	1.872(9)	Mo(1)–η^5Cp	1.995(9)	Mo(1)–η^3Cp	2.044(10)	Mo(1)–η^5Cp	1.926(8)
Mo(1)–η^4Cp	2.013(10)	Mo(1)–P(2)	2.455(2)	Mo(1)–C(2)	1.939(12)	Mo(1)–N(2)	2.153(6)
Mo(1)–P(2)	2.479(2)	P(1)–C(121)	1.843(6)	P(1)–C(112)	1.785(11)	N(1)–C(11)	1.141(8)
P(1)–C(121)	1.835(9)	P(2)–C(221)	1.841(6)	P(1)–C(21)	1.828(8)	N(2)–C(21)	1.127(8)
P(2)–C(211)	1.855(9)	P(2)–C(211)	1.869(6)	C(2)–O(2)	1.159(12)	Mo(1)–$\eta^4C_6H_8$	1.872(7)
P(2)–C(221)	1.841(10)	Mo(1)–η^3Cp	1.980(8)	Mo(1)–η^5Cp	2.010(13)		
Mo(1)–η^5Cp	1.964(10)						
P(1)–Mo(1)–P(2)	78.16(8)	P(1)–Mo(1)–P(2)	78.45(6)	C(1)–Mo(1)–η^5 Cent	116.2	N(1)–Mo(1)–N(2)	81.2(2)
P(1)–Mo(1)–η^4 Cent	99.7	P(1)–Mo(1)–η^3 Cent	98.7	C(2)–Mo(1)–η^5 Cent	124.2	N(1)–Mo(1)–η^4 Cent	101.9
P(2)–Mo(1)–η^4 Cent	102.4	P(2)–Mo(1)–η^3 Cent	96.8	C(1)–Mo(1)–C(2)	82.3(4)	N(2)–Mo(1)–η^4 Cent	103.1
P(1)–Mo(1)–η^5 Cent	117.9	P(1)–Mo(1)–η^5 Cent	116.2	C(111)–P(1)–C(113)	107.5(5)	N(1)–C(11)–C(12)	178.2(8)
P(2)–Mo(1)–η^5 Cent	114.9	P(2)–Mo(1)–η^5 Cent	122.8	C(111)–P(1)–C(21)	110.3(4)	N(2)–C(21)–C(22)	179.1(8)
				C(113)–P(1)–C(21)	110.0(5)	N(1)–Mo(1)–η^5 Cent	111.3
				O(2)–C(2)–Mo(1)	177.1(10)	N(2)–Mo(1)–η^5 Cent	121.4
				C(1)–Mo(1)–η^3 Cent	98.1	C(11)–N(1)–Mo(1)	173.8(6)
				C(2)–Mo(1)–η^3 Cent	96.9	C(21)–N(2)–Mo(1)	172.3(6)
				C(112)–P(1)–C(113)	110.1(7)		
				C(112)–P(1)–C(21)	111.7(5)		
				C(111)–P(1)–C(112)	107.0(6)		
				O(1)–C(1)–Mo(1)	178.6(9)		

MoLL′ plane bisects the plane defined by the normals to the rings, in the diene derivatives there is an asymmetry, as defined in **c**, α and β being different, here respectively 57.6° and 69.7°. These values are very similar to those found in the complex $[CpMo(\eta^4\text{-}C_6H_8)(dppe)][PF_6] \cdot SO_4$ [28].

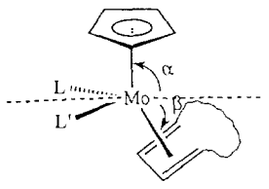

c

*2.3.2. Crystal structure of endo-CpMo(η^3-C_5H_7)(dppe) (**10**)*

The crystal structure of **10**, shown in Fig. 2, is similar to many other structures of $CpMo(\eta^3\text{-allyl})L_2$ complexes, e.g. $CpMo(\eta^3\text{-}C_3H_5)(CO)_2$ [32]. The coordination geometry around the Mo atom is pseudo tetrahedral like in **9**. The η^3-allyl fragment coordinates via C(21), C(22) and C(23) and has an *endo* conformation, the same found in $CpMo(\eta^3\text{-}C_8H_{13})(NO)(CO)$ [33], $(neomenthylCp)Mo(\eta^3\text{-}C_3H_5)(NO)(CO)$ [34], $(neomenthylCp)CpMo(\eta^3\text{-}C_3H_5)(NO)(I)$ [34], $CpMo(\eta^3\text{-}C_3H_5)(NO)(I)$ [32].

The allyl ligand is almost symmetric both in **10** (Mo–C(21) 2.285(6) Å, Mo–C(22) 2.179(6) Å, Mo–C(23) 2.272(7) Å) and in $CpMo(\eta^3\text{-}C_3H_5)(CO)_2$ [32]. The angle between the normals to the allylic plane and the Cp ring is 121.1(4)° and the fold angle of the bent $\eta^3\text{-}C_5H_7$ ring is 33.2(6)°.

The Mo–P distances are slightly shorter than those found in **9**. Again, steric interactions between the several rings are reflected in the short H...H intramolecular contacts. The plane containing the normals to the Cp and allyl ligands is almost perpendicular (92.3°) to the plane containing the two Mo–P bonds, and has the same angle found in **9** (92.3°).

*2.3.3. Crystal structure of [CpMo(η^3-$C_6H_8PMe_3$)$(CO)_2$]BF_4 (**24**)*

The crystal structure of $[CpMo(\eta^3\text{-}C_6H_8PMe_3)(CO)_2]^+$ is presented in Fig. 3 and the relevant bond distances and angles in Table 2.

The structural features of $\mathbf{24}^+$ are similar to those of the analogous $CpMo(\eta^3\text{-}C_6H_9)(CO)_2$ [1] with comparable C–Mo–C (82.3(4)° vs. 82.7(1)°) and internal allylic (115.7(9)° vs. 116.7(3)°) angles. In the allylic ligand the central atom C(23) (Mo–C(23) = 2.201(8) Å) is closer to the metal than the terminal carbons (Mo–C(22) = 2.358(7) Å and Mo–C(24) = 2.372(10) Å).

The angle between the normals to the Cp ring and the allyl plane is 138.8(10)°. The $\eta^3\text{-}C_6H_8PMe_3$ ring adopt a chair conformation with the PMe_3 substituent occupying an axial position and lying on the external

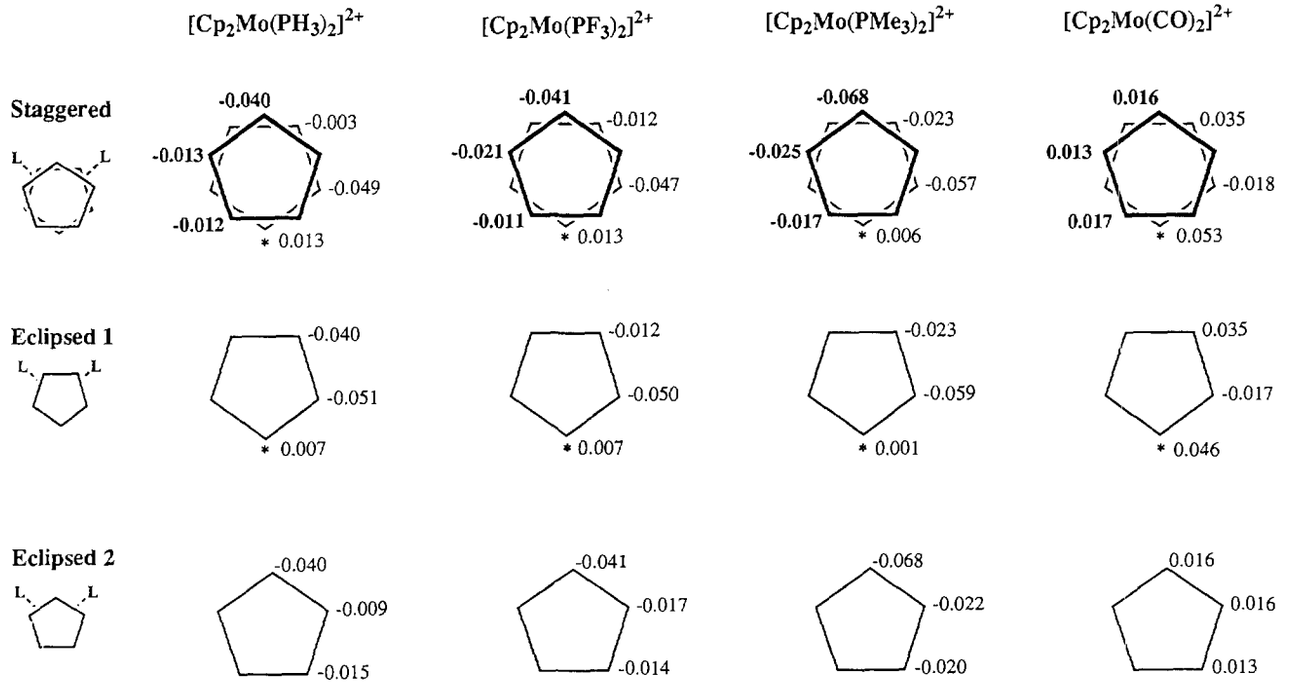

Fig. 5. Charges in the Cp carbon atoms for several $[Cp_2MoL_2]^{2+}$ complexes for three different arrangements of the rings.

face of the ring. Previous X-ray crystallographic studies made by Faller et al. [1], Green et al. [35], and Pearson et al. [36] showed that in cyclohexenyl–$CpMo(CO)_2$ complexes the six membered rings adopt a chair conformation regardless of substitution pattern. The α and β angles, defined in **c** above, are in this cation 49.8(6)° and 89.0(9)° respectively, differing much more than in **9**, as steric effects are not so important here.

2.3.4. Crystal structure of $[CpMo(\eta^4\text{-}C_6H_8)(NCMe)_2]BF_4$ (25)

The crystal structure of $[CpMo(\eta^4\text{-}C_6H_8)(NCMe)_2]^+$ is presented in Fig. 4. The most relevant bond angles and distances are in Table 2.

The structural features of the cyclohexadiene complex cation $\mathbf{25}^+$ are similar to those of the complex $\mathbf{9}^+$ and of $[CpMo(\eta^4\text{-}C_6H_8)(dppe)]PF_6 \cdot SO_4$ [28]. The angle between the normals to the planes of the Cp ring and that of the 4 olefinic carbons of the C_6H_8 ring, is 125.04(9)°. The fold angle of the C_6H_8 ring is 41.5(4)°.

The four olefinic carbon atoms are bonded to the metal in a rather asymmetric way; Mo–C112 = 2.318(7) Å, Mo–C(113) = 2.309(6) Å, Mo–C(114) = 2.277(7) Å, Mo–C(115) = 2.270(7) Å; C(112)–C(113) = 1.407(11) Å, C(113)–C(114) = 1.379(12) Å and C(114)–C(115) = 1.415(11) Å. The distances from the Mo to the diene (1.872(7) vs. 1.91 Å) and Cp planes (1.926(8) vs. 1.97 Å) are comparable to the corresponding ones found for complex $[CpMo(\eta^4\text{-}C_6H_8)(dppe)][PF_6] \cdot SO_4$.

The N atoms and the Mo atom lie in a plane that makes an angle of 91.9(3)° with the plane formed by the normals defined above. The Mo–N distances of 2.143(5) and 2.153(6) Å are comparable with other Mo–N distances of Cp_2MoL_2 complexes with N donor atom ligands [37].

2.4. Theoretical studies

In order to understand the nucleophilic attack patterns observed in the previously described reactions, extended Hückel calculations were performed [38,39]. The first question concerns the preference for the attack, which depends on the charge distribution. Although the absolute values of the charges cannot be trusted, the trends upon ligands substitution are indicative of their real changes. The model used consisted of a $[Cp_2MoL_2]^{2+}$ complex, ($L = PH_3$, PF_3, PMe_3, CO) and we analyzed the charges for these derivatives, considering three relative arrangements of the Cp ligands, namely, staggered, eclipsed with one short H...H contact (eclipsed 1) or eclipsed with two short H...H contacts (eclipsed 2). The charges are given in the Fig. 5, for the three arrangements of the four complexes.

These results indicate that there is a position of the Cp ring (marked with *) where positive charge concentrates, irrespective of the ligand L. It can be seen, however, that moving from a phosphine to a carbonyl has a remarkable effect upon the charges on the carbons of the Cp.

They become much more positive, as electron density is pushed in the carbonyls and out of the Cp rings. Changes form one phosphine to the other are less important.

In view of this charge distribution, one might expect that kinetically controlled nucleophilic attack of H^- would always be preferred in the marked position, suggesting an *endo*-$[CpMo(\eta^4\text{-}C_5H_6)L_2]^+$ conformation for the reaction product. This is confirmed by the geometry of the final complexes $[CpMo(\eta^4\text{-}C_5H_6)L_2]^+$ (**9**, L_2 = dppe; **11**, $L = PMe_3$). In the case of the carbonyl derivative both isomers are present in solution [18]. This led us to study the rearrangements of the $\eta^4\text{-}C_5H_6$ ligand in several $[CpMo(\eta^4\text{-}C_5H_6)L_2]^+$ species, ($L = CO$, PH_3, PMe_3, and PPh_2H) starting from the kinetically favoured *endo* conformation **a** and allowing the $\eta^4\text{-}C_5H_6$ ligand to rotate 180° in order to move to the *exo* conformation **b**. The geometries were not optimized, though the models were chosen in order to reproduce the experimental structures. This means that the calculated rotation barriers are probably too high.

These results show the influence of steric factors in preventing free rotation once the new diene is formed. The energy differences between *exo* and *endo* forms are very small, except for the bulkier phosphine. In this case, the rotation barrier is also too high to be easily overcome.

3. Discussion

Functionalization of cyclopentadiene rings is usually done by means of the deprotonation to $C_5H_5^-$ (Cp^-) followed by the reaction with electrophiles, E^+, to give C_5H_5E. Repeating this process from the latter molecule gives mixtures of 1,2 and 1,3 disubstituted products $C_5H_4E_2$ [11]. The double sequential nucleophilic addition of H^- to the Cp ring of $[Cp_2Mo(dppe)]^{2+}$ (**1**) seemed to offer an alternative to the preparation of 1,2 disubstituted C_5 rings from coordinated Cp since, according to the Davies–Green–Mingos rules, it yields a cyclopentenyl complex with both added substitutents on the same (external) face of the ring, as depicted in Scheme 2 for H^*. In the present case, the relatively rare nucleophilic addition to coordinated Cp rings is favoured by the high positive charge imparted to the Cp rings of the starting dication **1**.

For most of the dications tried, $[Cp_2MoL_2]^{2+}$, even the simpler double H^- addition was not feasible as they

give either incomplete (L_2 = en, **4**), irreproducible (L = CO, **3**) or untractable reactions (L_2 = dth, **5**). For the sake of comparison mention should be made to the reactions of the closely related species $[Cp_2Mo(NH_3)_2]^{2+}$ which readily gives Cp_2MoH_2 [40], and $[Cp_2Mo(SCH_2CHSMe)]^+$ which gives $Cp_2Mo(SCH_2CH_2SMe)(H)$ most presumably via initial H^- attack to the ring followed by H migration to metal as elegantly demonstrated by Cooper in the reaction of the related W complexes $[Cp_2W(SMe_2)X]^+$ with carbon nucleophiles (R^-) to give CpCp'WHX (Cp' = C_5H_5R) [40,41].

However, double H^- addition is facile, stepwise and reproducible for the phosphine dications $[Cp_2MoP_2]^{2+}$ **1** (P_2 = dppe) and **2** (P = PMe_3). In both cases only one conformer (rigid in solution at room temperature) was obtained for each of the complexes resulting from the first H^- addition step namely, *endo*-$[CpMo(\eta^4\text{-}C_5H_6)(dppe)]^+$ (**9**) and *endo*-$[CpMo(\eta^4\text{-}C_5H_6)(PMe_3)_2]^+$ (**11**). This conformation is imposed by the electronic properties of the substrate dication $[Cp_2MoP_2]^{2+}$. In fact, considering that H^- adds on to the external face of the Cp ring [14], and that such additions on 18-electron cations are kinetically and charge controlled reactions [7–9], the charges given in Fig. 5 suggest the initial formation of *endo*-$[CpMo(\eta^4\text{-}C_5H_6)P_2]^+$ from any dication $[Cp_2MoP_2]^{2+}$ as observed experimentally. The higher energy of the *exo*-**9** isomer and high *endo / exo* rotation barrier calculated for the model compound of **9**, $[Cp_2Mo(PPh_2H)_2]^{2+}$, (Table 3) are further arguments to prevent the formation *exo*-**9** isomer. Similar arguments based on the values of Fig. 5 and Table 3, suggest that H^- addition to the dication $[Cp_2Mo(CO)_2]^{2+}$ would originate the kinetically and thermodynamically controlled *endo*-$[CpMo(\eta^4\text{-}C_5H_6)(CO)_2]^+$. Experiment shows that both isomers interconvert and are present at room temperature. It seems, therefore, that the interconversion barrier is smaller for the CO complex when compared with the phosphine analogue **11** in contrast with the predictions based on the values in Table 3. In fact, the values calculated for the rotation barriers are only indicative and do not allow us to distinguish between the two isomers. A more detailed study of *exo / endo* conversions in $[CpMo(\eta^4\text{-diene})L_n]$ complexes addresses these questions by means of molecular mechanics calculations and will be published elsewhere [24].

Table 3
Relative energy between the *endo* and *exo* conformers and activation energy (ΔE) for their interconversion (eV)

Energy (eV)	*endo*	*exo*	ΔE
$[Cp_2Mo(CO)_2]^{2+}$	0.0	0.12	0.63
$[Cp_2Mo(PH_3)_2]^{2+}$	0.0	0.26	0.62
$[Cp_2Mo(PMe_3)_2]^{2+}$	0.0	0.10	0.64
$[Cp_2Mo(PPh_2H)_2]^{2+}$	0.0	1.15	5.00

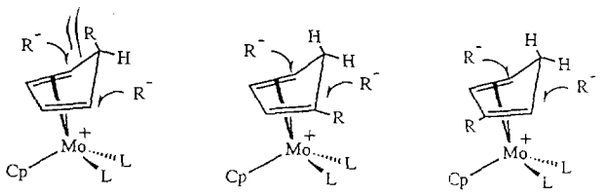

Scheme 5.

The second H^- addition occurs on *endo*-**9** and *endo*-**11** at the terminal diene C atom, according to the Davies–Green–Mingos rules as confirmed for the crystallographically characterized *endo*-$CpMo(\eta^3\text{-}C_5H_7)(dppe)$. Qualitatively, it is also clear that the latter addition is easier for the dppe complex **9** than for the electron richer PMe_3 analogue **11**.

Unfortunately, this reactivity was not reproduced with the carbon nucleophiles which was one of the initial goals of this work. In no case was double addition obtained upon reaction of $[Cp_2ML_2]^{2+}$ [L_2 = $(CO)_2$, dppe] with stabilized and unstabilized carbanions, e.g. $^-CH_2CN$, $^-CH_3$ under several experimental conditions. This means that the initially formed cyclopentadiene derivatives $[CpMo(\eta^4\text{-}C_5H_5R)L_2]^+$ do not undergo the expected addition of a carbon nucleophile. This strongly contrasts with the reactivity of the similar cyclohexadiene complexes $[CpMo(\eta^4\text{-}C_6H_7R)(CO)_2]^+$ (R = H, alkyl) which undergo stereo and regiospecific nucleophilic attack by hard carbon nucleophiles like Grignard reagents [1].

Two reasons may be held responsible for this result. The first one is the facile deprotonation of the C_5H_5R ring in the $[CpMo(\eta^4\text{-}C_5H_5R)L_2]^+$ complexes that leads to η^3–Cp complexes, e.g. $CpMo(\eta^3\text{-}C_5H_4R)L_2$, which undergo decomposition due to their high reactivity. Such deprotonations are very facile in the case of the L = CO derivatives as we have reported before [16–18]. The phosphine derivatives are less acidic but even considering that $[CpMo(\eta^4\text{-}C_5H_5R)(dppe)]^+$ does not react with NEt_3 like its CO congeners, it may not resist deprotonation by the more basic carbon nucleophiles. The second reason, we believe the most important, is the steric hindrance of the second nucleophilic addition caused by the presence of the first substituent on the *exo* C_5 position of the coordinated C_5H_5R ring as shown in **d**, Scheme 5. A similar dramatic decrease of the reactivity toward nucleophiles is observed in the nucleophilic additions to the cyclohexadienyl ring in complexes $[Mn(CO)(NO)(L)(\eta^5\text{-}C_6H_6R)]^+$ (**26**) when R is at the C-6 *exo* position [9]. In the absence of a

kinetically accessible addition pathway, decomposition is favoured by alternative reactions like deprotonation.

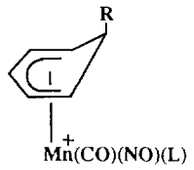

26

In agreement with this, all attempts to react $[CpMo(\eta^4\text{-}C_5H_6)L_2]^+$ (L = $(CO)_2$, dppe) with carbon nucleophiles led to decomposition with the exception of $LiCuMe_2$ which produced the cyclopentenyl derivatives $CpMo(\eta^3\text{-}C_5H_6Me)L_2$ under carefully controlled reaction conditions.

At this point one should also note that, even disregarding the acid–base and/or the steric arguments above, R^- addition to the independently prepared monosubstituted cyclopentadiene complexes, $[CpMo(\eta^4\text{-}C_5H_5R)L_2]^+$ [16–18], is no alternative for the synthesis of coordinated, disubstituted 1,2-$C_5H_5R_2$ rings. In fact, as demonstrated in the case of $[CpMo(\eta^4\text{-}C_5H_5Me)(CO)_2]^+$ [16–18], several position isomers of the diene ring are present which invalidate the desired regioselectivity control. As depicted in Scheme 5, attack at the terminal C atoms of the diene would lead to mixtures of isomers except in the case of **d** where only the 1,2 product is formed. Isomer **e** leads to 1,1 and 1,3 disubstituted rings and isomer **f** to 1,2 and 1,3 disubstituted rings. The situation represented in **d** is precisely the one predicted by applying the Davies–Green–Mingos rules to double sequential R^- addition to $[Cp_2MoL_2]^+$.

The addition of group 5 and 6 nucleophiles to both $[Cp_2Mo(dppe)]^{2+}$ and $[Cp_2Mo(CO)_2]^{2+}$ also failed to give double addition products. Excess PhS^- leads to $Cp_2Mo(SPh)_2$ by metal disubstitution. However, the *exo* substituted monoadducts $[CpMo(\eta^4\text{-}C_5H_5SMe)(dppe)]^+$ and $[CpMo(\eta^4\text{-}C_5H_5PMe_3)(CO)_2]^+$ are readily formed from the corresponding dications. Since nucleophilic additions readily take place onto the *unsubstituted* diene of complexes $[CpMo(\eta^4\text{-}C_5H_6)(CO)_2]^+$ to give $Cp'Mo(\eta^3\text{-}C_5H_6SPh)(CO)_2$ (Cp′ = Cp, Ind) as well as $[CpMo(\eta^3\text{-}C_5H_6PMe_3)(CO)_2]^+$ and $[CpMo(\eta^3\text{-}C_6H_8PMe_3)(CO)_2]^+$, the failure to observe a double sequential nucleophilic addition to the cyclopentadienyl ring of $[Cp_2MoL_2]^{2+}$, in all cases except for H^-, is most certainly due to steric hindrance

In contrast to the well understood regiochemistry of the Davies–Green–Mingos rules, electrophilic and oxidative reactions of organometallic complexes are much less predictable although they are necessary steps in many metal promoted diene functionalization methods. Considering the electrophilic H^- abstractions with Ph_3C^+, all the cyclopentadiene complexes $[CpMo(\eta^4\text{-}C_5H_6)L_2]^+$ react similarly producing the corresponding dicationic derivatives $[Cp_2MoL_2]^{2+}$ regardless of L. The reaction is extensive to other oxidants namely Cl_2 and Br_2. However, similar abstractions do not take place from the cyclohexadiene or cycloheptatriene complexes $[CpMo(\eta^4\text{-}C_6H_8)(CO)_2]^+$ or $[CpMo(\eta^4\text{-}C_7H_8)(CO)_2]^+$ probably due to the instability of the open pentadienyl complexes that would result, e.g. $[CpMo(\eta^5\text{-}C_6H_7)(CO)_2]^{2+}$ and $[CpMo(\eta^5\text{-}C_7H_7)(CO)_2]^{2+}$ respectively. The aromatization of the cyclopentadienyl ring, absent in the latter hypothetic compounds, certainly provides the thermodynamic driving force for the process. Mechanistically, this abstraction seems to involve acid/base H^- transfer of the *exo* methylene hydrogen of the C_5H_6 ring to the Ph_3C^+ cation since the cyclic voltammogram (CV) of the cation $[CpMo(\eta^4\text{-}C_5H_6)(CO)_2]^+$ does not present any oxidation wave within the solvent limits (NCMe, CH_2Cl_2). However, a redox initiated mechanism involving sequential 1-electron oxidation of the cyclopentadiene cation followed by $H^{\cdot}$ abstraction cannot be ruled out in the case of the electron richer and oxidizable phosphine analogues **9** and **11**. Indeed, $[CpMo(\eta^4\text{-}C_5H_6)(dppe)]^+$ reacts with ferricenium to produce $[Cp_2Mo(dppe)]^{2+}$ and ferrocene although only in moderate yield. The importance of single electron step mechanisms seems to be marginal in the reverse nucleophilic additions to π hydrocarbon rings of $[M(\eta^x\text{-hydrocarbon})(CO)_n]^+$ electrophiles [9].

In the group of the neutral cyclopentenyl complexes $CpMo(\eta^3\text{-}C_5H_7)L_2$, reaction of Ph_3C^+ with $CpMo(\eta^3\text{-}C_5H_7)(CO)_2$ and $CpMo(\eta^3\text{-}C_5H_7)(PMe_3)_2$ gives the corresponding $[CpMo(\eta^4\text{-}C_5H_6)L_2]^+$. These results parallel the reaction of the cyclohexenyl complexes $CpMo(\eta^3\text{-}C_6H_8R)(CO)_2$ (R = H, alkyl) with Ph_3C^+ that gives the cyclohexadiene complexes $CpMo(\eta^4\text{-}C_6H_7R)(CO)_2]^+$ [1]. Quite unexpectedly, however, reaction of Ph_3C^+ with $CpMo(\eta^3\text{-}C_5H_7)$dppe does not give $[CpMo(\eta^4\text{-}C_5H_6)(dppe)]^+$ (**9**). Instead, a mixture of 60% $[CpMo(dppe)_2]^{2+}$ and 30% of $[Cp_2Mo(dppe)]^{2+}$ is formed without traces of **9**.

The CV data in Table 1 show that all the $CpMo(\eta^3\text{-}C_5H_7)L_2$ complexes are irreversibly oxidized in contrast to their parent allyl $CpMo(\eta^3\text{-}C_3H_5)(CO)_2$. This fact favours the consideration of a simple acid/base H^- abstraction mechanism which does not involve any unstable radical-cation species $[CpMo(\eta^3\text{-}C_5H_7)L_2]^{\cdot}$. In our opinion, the diverging behaviour of the dppe derivative $CpMo(\eta^3\text{-}C_5H_7)$dppe (**10**) can be explained assuming steric hindrance in the formation of the transition state for acid/base H^- abstraction, due to the bulk of the Ph substituents of the dppe ligand. Short intramolecular contacts between these phenyl hydrogens and

the C_5H_7 ring are found in the crystal structure of **10** (Fig. 2). Therefore, in the absence of this simple H^- transfer pathway, electron transfer takes place to give most probably the radical-cation $[CpMo(\eta^3\text{-}C_5H_7)dppe]^{\cdot+}$ which decays (dismutation, C_5H_7 radical loss, etc.) to the final products. The irreproducible reaction of $CpMo(\eta^3\text{-}C_5H_7)$dppe with ferricenium most certainly follows related pathways as ferrocene is formed in the process.

4. Conclusions

The cyclopentadiene complexes $[CpMo(\eta^4\text{-}C_5H_5R)L_2]^+$ are isolated from the dications $[Cp_2MoL_2]^{2+}$ (L = CO, PMe_3, dppe) and several nucleophiles (R^-) depending on L (L = dppe, R = H, CH_3, CH_2CN, CH_2PPh_3, SMe; L = CO, R = H, CH_3, SPh, PMe_3; L = PMe_3, R = H). Only one rigid conformer is obtained in each of the phosphine containing complexes, while the CO derivatives are fluxional in all cases. EHMO calculations correctly predict the kinetically controlled isomers but are not sufficiently accurate to interpret the fluxional behaviour.

Even with large excess of R^-, the synthetically useful sequential double nucleophilic addition of R^- to one of the Cp rings of those dications to form the cyclopentenyl complexes $CpMo(\eta^3\text{-}1,2\text{-}C_5H_5R_2)L_2$ in a regio and stereospecific way was only achieved for the hydride (R = H; L = CO, PMe_3, dppe). Steric hindrance caused by the first R substituent seems to block the reactivity of the coordinated cyclopentadiene in $[CpMo(\eta^4\text{-}C_5H_5R)L_2]^+$. This contrasts with the well established high reactivity of the cyclohexadiene analogues $[CpMo(\eta^4\text{-}C_6H_7R)(CO)_2]^+$ towards a range of nucleophiles.

On the other hand, the reverse H^- abstractions (Ph_3C^+) from $[CpMo(\eta^4\text{-}C_5H_6)L_2]^+$ and $CpMo(\eta^3\text{-}C_5H_7)L_2$ are facile in all cases except for $CpMo(\eta^3\text{-}C_5H_7)$(dppe) where steric bulk seems to favour (uncontrolled) electron transfer reactions.

5. Experimental details

All experiments were carried out under an atmosphere of argon by Schlenk techniques. Diethyl ether, THF and pentane were dried by distillation from Na/benzophenone. Acetonitrile was dried over CaH_2 and distilled after refluxing several hours over CaH_2–P_2O_5. Dichloromethane was distilled from CaH_2. Acetone was distilled and kept over 4 Å molecular sieves.

Microanalyses were performed by Eng. João P. Lopes in our laboratories (ITQB). ^{1}H NMR spectra were obtained with a Bruker CXP 300 spectrometer. Infrared spectra were recorded on a Perkin-Elmer 457 and on a Unican Mattson Mod 7000 FTIR spectrophotometer using KBr pellets.

PMe_3 [42], $LiCuMe_2$ [43], $LiCH_2CN$ [44], $[CpMo(\eta^4\text{-}C_5H_6)(dppe)]PF_6$ [14], $[Cp'Mo(\eta^4\text{-}C_5H_6)(CO)_2]BF_4$(Cp' = Cp, Ind) [16–18] $CpMo(\eta^3\text{-}C_5H_7)$(dppe) [14], $[Cp_2Mo(CO)_2][BF_4]_2$ [16–18] and $[CpMo(\eta^4\text{-}C_6H_8)(CO)_2]BF_4$ [1] were prepared as described previously.

6. Electrochemistry

The electrochemical instrumentation consisted of a PAR 173 potentiometer, a PAR 175 voltage programmer and a Houston Instruments Omnigraphic 2000 X-T or a EG and G Princeton Applied Research Potenciostat Model 273A, connected to the data acquisition software (EG and G PAR Electrochemical Analysis Model 273 Version 3.0).

The reference electrode, a calomel electrode containing a saturated solution of potassium chloride, was calibrated using a solution of ferrocene (1mM) containing 0.1M $LiClO_4$ for which the ferricinium/ferrocene potential was in agreement with the literature value [45].

The working electrodes were a 2 mm piece of Pt wire and the auxiliary electrode a Pt wire coil. The voltammetric experiments were performed at room temperature, in an argon atmosphere, in a standard single-compartment three electrode design (PAR polarographic cell). Solutions used were 1mM in solute and 0.1M in the supporting electrolyte, tetrabutylammonium hexafluorophosphate (Sigma Chemical Co.).

Solvents were dried as previously described. Solutions were degassed with dry nitrogen (or argon) before each experiment and an inert atmosphere was maintained over the solution.

7. Experimental

7.1. Preparation of $[Cp_2Mo(dppe)][BFu]_2$ (1)

A suspension of Cp_2MoI_2 (0.96 g, 2 mmol) in NCMe was treated with dppe (0.99 g, 2.5 mmol) and $TlBF_4$ (1.16 g, 4 mmol). The mixture was refluxed for 3 h. The resulting orange solution that formed was separated from TlI by filtration and evaporated to dryness to give a powder. Yellow crystals were obtained from recrystallization with NCMe/Et_2O. (Yield, 87%.) EA, IR (KBr) and ^{1}H NMR data are in agreement with Ref. [14].

7.2. Preparation of $[Cp_2Mo(PMe_3)_2]^{2+}$ (PF_6^- or BF_4^-) (2)

7.2.1. Method a

Treatment of a suspension of Cp_2MoI_2 (0.19 g, 0.40 mmol) in acetone with PMe_3 (0.80 ml, 8 mmol) and

$TlPF_6$ (0.29 g, 0.82 mmol) caused immediate change in the colour from green to yellow. After stirring for 2 h the solvent was removed and the residue extracted with acetonitrile at 50°C. The resulting yellow solution was evaporated to dryness to give a powder. Yellow crystals were obtained from recrystallization with acetone/ethanol. (Yield, 84%.)

7.2.2. Method b

A solution of $[CpMo(\eta^4\text{-}C_5H_6)(PMe_3)_2]BF_4$ (0.12 g, 0.28 mmol) in dichloromethane was treated with a solution of Ph_3CBF_4 (0.09 g, 0.28 mmol) in the same solvent. After 30 min of stirring, the yellow powder that formed was filtered off and washed with dichloromethane and ether. (Yield, 85%.) Anal. Found: **C** 34.70; **H** 5.10. Calc. for $C_{16}H_{28}B_2F_8P_2Mo$: **C** 34.82; **H** 5.11%. Selected **IR** (KBr, cm^{-1}): ν 3140; 2930; 1440; 1320; 1050. ^{1}**H** NMR (CH_3CN-d_3, 100 MHz, r.t., δ ppm): 5.57 (t, 5H, [$^3J_{PH}$ = 2.5 Hz], Cp); 1.66 (d, 9H, PMe_3).

7.3. Preparation of $[Cp_2Mo\{P(OMe)_3\}_2][BF_4]_2$ (4)

A suspension of $[Cp_2Mo(CO)_2][BF_4]_2$ (0.23 g, 0.50 mmol) in dichloromethane was treated with excess $P(OMe)_3$ (3 ml), refluxed and irradiated with a 60 W tungsten bulb for 2 h. The resulting yellow solution was evaporated to yield an oil which was solidified by adding ethanol. The yellow powder was washed with ether and recrystallized from acetone/ethanol. (Yield, 70%.) Anal. Found: **C** 29.70; **H** 4.21. Calc. for $C_{16}H_{28}B_2F_8O_6P_2Mo$: **C** 29.66; **H** 4.36%. Selected **IR** (KBr, cm^{-1}): ν 3103; 2960; 1440; 1417; 1055. ^{1}**H** NMR (CH_3CN-d_3, 100 MHz, r.t., δ ppm): 5.70 (s, 10H, Cp); 3.87 (t, 18H, $P(OMe)_3$).

7.4. Preparation of $[Cp_2Mo(NCMe)(PMe_3)]^{2+}$ (PF_6^- or BF_4^-) (7)

A solution of Cp_2MoI_2 (0.19 g, 0.40 mmol) in NCMe was treated with PMe_3 (0.5 ml, 5 mmol) and $TlBF_4$ or $TlPF_6$ (0.80 mmol). The orange solution was filtered to remove TlI and the solvent evaporated under vacuum. The residue was washed with Et_2O and recrystallized from acetone/Et_2O. The yellow crystals were isolated in 85% yield. Anal. Found for $[Cp_2Mo(NCMe)(PMe_3)][BF_4]_2$: **C** 36.44; **H** 5.28; **N** 2.41. Calc. for $C_{18}H_{31}B_2F_8NPMo$: **C** 36.46; **H** 5.27; **N** 2.36%. **IR** (KBr, cm^{-1}): ν 3100, 2930, 2280, 1425, 1320, 1050. ^{1}**H** NMR (CH_3CN-d_3, 300 MHz, r.t., δ ppm): 5.38 (d, 5H, [$^3J_{PH}$ = 3.2 Hz], Cp); 1.91 (s, 3H, NCMe); 1.67 (d, 9H, [$^3J_{PH}$ = 14.7 Hz], PMe_3).

7.5. Preparation of $[Cp_2Mo(H)PMe_3]I$ (8)

A solution of $Cp_2Mo(H)I$ (0.15 g, 0.44 mmol) in NCMe was treated with PMe_3 (0.04 ml, 0.44 mmol). After stirring for 1 h 30 min the solution became orange and the solvent was removed under vacuum. Part of the residue was extracted with CH_2Cl_2 and the solution evaporated to dryness. Recrystallization from NCMe afforded yellow crystals of $[Cp_2Mo(H)PMe_3]I$ in 30% yield. The undissolved residue was extracted in NCMe. Upon concentration and cooling yellow crystals separated (70% yield) and were shown to be the I^- salt of $[Cp_2Mo(PMe_3)_2]^{2+}$ by IR and ^{1}H NMR spectroscopy. Anal. Found: **C** 36.20; **H** 4.65; **Mo** 22.29. Calc. for $C_{13}H_{20}IPMo$: **C** 36.30; **H** 4.69; **Mo** 22.31%. Selected **IR** (KBr, cm^{-1}): ν 3060, 2960, 2900, 1440, 1300. ^{1}**H** NMR (CH_3CN-d_3, 90 MHz, r.t., δ ppm): 5.07 (d, 10H, [$^3J_{PH}$ = 12.0 Hz], Cp); 1.50 (d, 9H, [$^2J_{PH}$ = 36 Hz], PMe_3); −8.90 (d, 1H, [$^2J_{PH}$ = 144 Hz], Mo–H).

7.6. Preparation of $[CpMo(\eta^4\text{-}C_5H_6)(PMe_3)_2]BF_4$ (11)

7.6.1. Method a

A solution of $[Cp_2Mo(PMe_3)_2][BF_4]_2$ (0.18 g, 0.33 mmol) in NCMe was allowed to react with 1 eq. g of $NaBH_4$ (0.01 g, 0.33 mmol) for 1 h at room temperature. The resulting yellow solution was evaporated to dryness and the residue extracted with CH_2Cl_2. Slow addition of diethyl ether produced yellow crystals in 79% yield.

7.6.2. Method b

A solution of $CpMo(\eta^3\text{-}C_5H_7)(PMe_3)_2$ (0.13 g, 0.34 mmol) in dichloromethane was treated with a solution of Ph_3CBF_4 (0.11 g, 0.34 mmol) in the same solvent. After 30 min of stirring, the solvent was evaporated and the residue washed with ether. (Yield, 85%.) Anal. Found: **C** 41.26; **H** 6.22. Calc. for $C_{16}H_{29}BF_4P_2Mo$: **C** 41.23, **H** 6.27%. Selected **IR** (KBr, cm^{-1}): ν 3100, 2980, 2920, 2270, 1425, 1300, 1050. ^{1}**H** NMR (CH_2Cl_2-d_2, 300 MHz, r.t., δ ppm): 5.22 (m, 2H, H^{2-3}); 4.91 (t, 5H, Cp, [$^3J_{PH}$ = 1,6 Hz]); 4.04 (d, 1H, [$^2J_{HH}$ = 11.8 Hz], H_{exo}); 2.96 (br, 2H, $H^{1/4}$); 2.60 (d, 1H, [$^2J_{HH}$ = 11.8 Hz], H_{endo}); 1.31 (t, 18H, [$^3J_{PH}$ = 3.3 Hz] PMe_3).

7.7. Preparation of $CpMo(\eta^3\text{-}C_5H_7)(PMe_3)_2$ (12)

$[CpMo(\eta^4\text{-}C_5H_6)(PMe_3)_2]BF_4$ (0.06 g, 0.14 mmol) was suspended in THF and excess $LiAlH_4$ was added. The resulting solution was stirred for 1 h. The unreacted $LiAlH_4$ was destroyed with 1 ml of propanol-2 and a few drops of water. The solution was evaporated and the residue extracted with pentane. The solvent was removed in vacuum. The product was obtained in 75% yield after sublimation at 100°C (10^{-4} mm Hg). Anal. Found: **C** 50.52; **H** 7.94. Calc. for $C_{16}H_{30}P_2Mo$: **C** 50.53; **H** 7.95%. **IR** (KBr, cm^{-1}): ν 3100, 2980, 2920, 1425, 1280. **MS**: m/z 382 (M^+), 314, 230, 76. ^{1}**H** NMR (C_6H_6-d_6, 300 MHz, r.t., δ ppm): 4.10 (s,

5H, Cp); 2.76 (d, 2H, [$^3J_{HH}$ = 8.16 Hz], $H^{4/6}$); 2.59 (m, 1H, [$^3J_{PH}$ = 10.4 Hz], H^2); 2.28 (c, 2H [$^3J_{HH}$ = 5.8 Hz, $^3J_{PH}$ = 2.9 Hz], $H^{1/3}$); 1.57 (d, 2H, [$^3J_{HH}$ = 8.2 Hz], $H^{5/7}$); 0.86 (t, 18H, [$^3J_{PH}$ = 2.6 Hz], PMe_3).

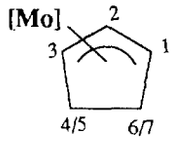

7.8. Preparation of $CpMo(\eta^3\text{-}C_5H_7)(CO)_2$ (12a)

7.8.1. Method a

Addition of $LiAlH_4$ (0.05 g, 1.38 mmol) to a suspension of $[Cp_2Mo(CO)_2][BF_4]_2$ (0.21 g, 0.46 mmol) in THF caused instantaneous dissolution of the compound to afford a yellow-green solution which was taken to dryness after the destruction of the unreacted $LiAlH_4$ with a few drops of water. The residue was extracted with ether to give an oil which was then extracted with hexane to afford the yellow microcrystalline compound in 50% yield.

7.8.2. Method b

Addition of $LiAlH_4$ (0.12 g, 3.16 mmol) to a suspension of $[CpMo(\eta^4\text{-}C_5H_6)(CO)_2]BF_4$ (0.40 g, 1.08 mmol) in THF caused instantaneous dissolution of the compound to afford a yellow solution which was taken to dryness after the destruction of the unreacted $LiAlH_4$ with water (2 ml). The residue was extracted with pentane to give the yellow microcrystalline compound in 80% yield. EA, IR (KBr) and ^{1}H NMR data are in agreement with Ref. [25].

7.9. Preparation of $CpMo(\eta^3\text{-}C_6H_9)(CO)_2$ (12b)

Addition of $LiAlH_4$ (0.12 g, 3.16 mmol) to a suspension of $[CpMo(\eta^4\text{-}C_6H_8)(CO)_2]BF_4$ (0.30 g, 0.78 mmol) in THF caused instantaneous dissolution of the compound to afford a yellow solution which was taken to dryness after the destruction of the unreacted $LiAlH_4$ with water (2 ml). The residue was extracted with pentane to give the yellow microcrystalline compound in 58% yield. EA, IR (KBr) and ^{1}H NMR data are in agreement with Ref. [1].

7.10. Preparation of $[CpMo(\eta^4\text{-}C_5H_6)(en)]PF_6$ (13)

A suspension of $[Cp_2Mo(en)]I_2$ (0.54 g, 1 mmol) in 1,2 dimethoxyethane (20 ml) was treated with excess $NaBH_4$ (0.1 g) at room temperature. After stirring for 15 min as the precipitate turned cherry-red, the solvent was removed under vacuum and the residue washed with water (2 × 5 ml) to remove the $NaBH_4$ excess. The compound was suspended in acetone (15 ml) and treated with excess $TlPF_6$. After stirring for 15 min, as TlI precipitated, the cherry-red acetone solution was filtered and EtOH (15 ml) added. Crystals were obtained by evaporation of the solvent. Anal. Found: **C** 33.60; **H** 4.60; N 6.40. Calc. for $C_{12}H_{19}N_2PF_6Mo$: **C** 33.40; **H** 4.40; **N** 6.50%. Selected **IR** (KBr, cm^{-1}): ν 3370; 3325; 2955; 1465; 1455; 1045; 880; 840.

7.11. Preparation of $[CpMo(\eta^4\text{-}C_5H_5Me)(dppe)]PF_6 \cdot CH_2Cl_2$ (14)

MeLi (1.1 ml, 1.4 mmol of a solution 1.29M in Et_2O) was slowly added, at 0°C, to a CuI suspension (0.11 g, 0.60 mmol) in Et_2O. The reaction mixture was allowed to react for 10 min until the precipitate initially formed was dissolved. $[Cp_2Mo(dppe)][PF_6]_2$ (0.18 g, 0.20 mmol) was added to the solution of $LiCuMe_2$ at −30°C, and stirred for 3 h at room temperature. The unreacted $LiCuMe_2$ was destroyed at −30°C with a few drops of ethanol. The solvent was removed in vacuum, the residue washed with Et_2O and extracted with CH_2Cl_2. Cooling at −20°C the concentrated extract gave the product as yellow crystals in 72% yield. Anal. Found: **C** 52.01; **H** 4.47; **P** 10.54. Calc. for $C_{38}H_{39}Cl_2F_6P_3Mo$: **C** 52.48; **H** 4.51; **P** 10.69%. Selected **IR** (KBr, cm^{-1}): ν 3100; 3050; 1475; 1435; 1425; 830; 750; 700. ^{1}**H** NMR (CH_2Cl_2-d_2, 300 MHz, r.t., δ ppm): 6.80–7.60 (m, 20H, Ph); 4.84 (s, 5H, Cp); 4.54 (dt, 2H, [$^3J_{PH}$ = 11.6 Hz], H^2, H^3); 3.25 (br, 2H, H^1, H^4); 3.12 (c, 4H, CH_2 of dppe); 2.53 (m, 1H, H^5); 0.40 (d, 3H, [$^3J_{HH}$ = 3.0 Hz], Me).

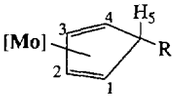

7.12. Preparation of $[CpMo(\eta^4\text{-}C_5H_5CH_2CN)(dppe)]PF_6 \cdot CH_2Cl_2$ (15)

NCMe (54.70 ml, 1.00 mmol) was added to a solution of ^{n}BuLi (1.00 mmol, 0.62 ml of a 1.6M solution) in THF at −70°C. $[Cp_2Mo(dppe)][PF_6]_2$ (0.17 g, 0.18 mmol) was added to the suspension of $LiCH_2CN$ in THF, and stirred for 2 h at room temperature. The unreacted $LiCH_2CN$ was destroyed with 2 ml of ethanol. The solvent was evaporated. After washing with Et_2O (3 × 10 ml) the residue was extracted with CH_2Cl_2. Slow addition of pentane to the concentrated extract gave the product as a yellow microcrystalline powder in 70% yield. Anal. Found: **C** 52.01; **H** 4.37; **N** 1.31. Calc. for $C_{39}H_{38}Cl_2F_6NP_3Mo$: **C** 52.37; **H** 4.28; **N** 1.56%. Selected **IR** (KBr, cm^{-1}): ν 3080, 3050, 2960, 2940, 2250, 1475, 1440, 1435, 1425, 830, 750, 700. ^{1}**H** NMR

(CH_2Cl_2-d_2, 300 MHz, r.t., δ ppm): 6.79–7.55 (m, 20H, Ph); 4.88 (s, 5H, Cp); 4.64 (dt, 2H, [$^3J_{PH}$ = 11.8 Hz], H^2, H^3); 3.27 (br, 2H, H^1, H^4); 3.12 (c, 4H, CH_2 of dppe); 2.79 (m, 1H, H^5); 1.69 (d, 2H, [$^3J_{HH}$ = 5.0 Hz], CH_2CN).

7.13. Preparation of [CpMo(η^4-$C_5H_5CH_2PPh_3$)(dppe)]$PF_6 \cdot CH_2Cl_2$ (16)

Addition of $[Cp_2Mo(dppe)][PF_6]_2$ (0.17 g, 0.19 mmol) to a solution of CH_2PPh_3 [46] in THF caused, after 4 h stirring, the precipitation of a yellow solid. This was filtered off and recrystallized from CH_2Cl_2. Cooling the concentrated extract gave the product as a yellow powder in 68% yield. Anal. Found: **C** 52.71; **H** 4.19; **Mo** 0.74. Calc. for $C_{56}H_{53}Cl_2F_{12}P_6Mo$: **C** 52.72; **H** 4.19; **Mo** 0.75%. Selected **IR** (KBr, cm^{-1}): ν 3070; 2060; 1475; 1435; 1425; 750; 700. ^{1}**H** NMR (CH_2Cl_2-d_2, 300 MHz, r.t., δ ppm): 6.77–7.85 (m, 20H, Ph + m, 15H, Ph); 4.74 (s, 5H, Cp); 4.66 (dt, 2H, [$^3J_{PH}$ = 11.8 Hz], H^2, H^3); 3.16 (c, 4H, CH_2 of dppe); 2.92 (br, 2H, H^1, H^4); 2.68 (m, 1H, H^5); 2.46 (dd, 2H, [$^3J_{HH}$ = 6.0, $^2J_{PH}$ = 11.9 Hz], CH_2PPh_3).

7.14. Preparation of CpMo(η^3-C_5H_6Me)(dppe) (17)

MeLi (3.2 ml, 4.1 mmol of a solution 1.6M in Et_2O) was slowly added, at 0°C, to a CuI suspension (0.34 g, 1.77 mmol) in ether. The reaction mixture was allowed to react for 10 min until the precipitate initially formed was dissolved. [CpMo(η^4-C_5H_6)(dppe)]BF_4 (0.27 g, 0.59 mmol) was added to the $LiCuMe_2$ solution at −30°C, and stirred for 3 h at room temperature. The unreacted $LiCuMe_2$ was destroyed at −30°C with a few drops of methanol. The reaction mixture was evaporated to dryness and the residue extracted with hexane. Yellow crystals were obtained in 40% yield by layering hexane onto a solution of Et_2O. Anal. Found: **C** 69.05; **H** 6.39. Calc. for $C_{37}H_{38}P_2Mo$: **C** 69.37; **H** 5.98%. Selected **IR** (KBr, cm^{-1}): ν 2965, 1483, 1433, 743, 694. ^{1}**H** NMR (C_6H_6-d_6, 300 MHz, r.t., δ ppm): 7.03–6.71 (m, 20H, Ph); 5.57 (s, 5H, Cp); 4.24 (s, 1H); 2.39 (s, 1H); 1.91 (t, 4H, CH_2 of dppe); 1.68–1.51 (m, 1H, $H^{4/5}$); 1.19–1.13 (m, 1H, $H^{4/5}$); 0.55 (d, 3H, Me).

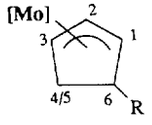

7.15. Preparation of CpMo(η^3-C_5H_6Me)$(CO)_2$ (18)

MeLi (1.6 ml, 2.0 mmol of a solution 1.6M in Et_2O) was slowly added, at 0°C, to a CuI suspension (0.17 g, 0.88 mmol) in Et_2O. The reaction mixture was allowed to react for 10 min until the initially formed precipitate was dissolved. [CpMo(η^4-C_5H_6)$(CO)_2$]BF_4 (0.11 g, 0.29 mmol) was added to the $LiCuMe_2$ solution at −30°C, and stirred for 2 h at room temperature. The unreacted $LiCuMe_2$ was destroyed at −30°C with a few drops of methanol. The reaction mixture was evaporated to dryness and the residue extracted with a mixture of hexane/ Et_2O to give a yellow powder. (Yield, 60%.) Anal. Found: **C** 51.96; **H** 4.71. Calc. for $C_{13}H_{14}O_2Mo$: **C** 52.36; **H** 4.73%. Selected **IR** (KBr, cm^{-1}): 1925, 1859, vs, ν(CO). ^{1}**H** NMR ($CHCl_3$-d_1, 300 MHz, r.t., δ ppm): 5.21 (s, 5H, Cp), 4.16 (t, 1H), 3.62 (q, 1H), 3.51 (t, 1H), 1.86–1.72 (m, 2H, $H^{4/5}$ + 1H), 1.48–1.40 (m, 1H, $H^{4/5}$), 0.93 (d, 3H, Me).

7.16. Preparation of [CpMo(η^4-C_5H_5SMe)(dppe)]PF_6 (19)

A suspension of $[Cp_2Mo(dppe)]_2[PF_6]_2$ (0.35 g, 0.38 mmol) in THF was treated with excess of NaSMe (0.10 g, 1.40 mmol) and stirred for 50 h. The solution was filtered and yellow crystals precipitated by removal of the solvent. Those crystals were washed with water to remove some remaining NaMeS and recrystallized from CH_2Cl_2/Et_2O. Anal. Found: **C** 53.8; **H** 4.8. Calc. for $C_{37}H_{37}SP_3F_6Mo$: **C** 54.4; **H** 4.6%. Selected **IR** (KBr, cm^{-1}): ν 3120; 3080; 2970; 2920; 1485; 1435; 1095; 875; 840; 750; 740. ^{1}**H** NMR (Me_2CO-d_6, 300 MHz, r.t., δ ppm): 7.00–8.00 (m, 20*H*, Ph); 5.18 (t, 5*H*, Cp); 4.83 (d, 2H, $H^{2/3}$); 3.83–3.18 (m, 7H, $H^{1/4}$ + H^5 + CH_2 of dppe); 1.72 (s, 3H, Me). Ω_M (NO_2Me) = 83.3 × 10^{-3}M.

7.17. Preparation of [CpMo(η^4-$C_5H_5PMe_3$)$(CO)_2$][BF_4]$_2$ (20)

Addition of excess PMe_3 (0.30 ml) to a suspension of $[Cp_2Mo(CO)_2][BF_4]_2$ (0.10 g, 0.22 mmol) in CH_2Cl_2 (15 ml) caused change of colour from white to yellow. After stirring for 2 h the precipitate was filtered off, washed with Et_2O and dried. The product was recrystallized from acetone/ethanol. (Yield, 77%.) Anal. Found: **C** 33.91; **H** 3.51. Calc. for $C_{15}H_{19}B_2F_8O_2PMo$: **C** 33.88; **H** 3.60%. Selected **IR** (KBr, cm^{-1}): 2058; 2010, vs, ν(CO). ^{1}**H** NMR (CH_3CN-d_3, 300 MHz, r.t., δ ppm): *isomer a*: 6.39 (t, 2H, $H^{2/3}$); 5.92 (s, 5H, Cp); 4.23 (t, 2H, $H^{1/4}$); 1.82–1.75 (dd 1H, H^5); 1.65 (d, 9H, PMe_3). *Isomer b*: 6.07(t, 2H, $H^{2/3}$); 5.92 (s, 5H, Cp); 4.38 (t, 2H, $H^{1/4}$); 1.82–1.75 (dd, 1H, H^5); 1.65 (d, 9H, PMe_3).

7.18. Preparation of CpMo(η^3-C_5H_6SPh)$(CO)_2$ (21)

Addition of excess NaPhS (0.08 g, 0.60 mmol) to a solution of [CpMo(η^4-C_5H_6)$(CO)_2$]BF_4 (0.24 g, 0.65 mmol) in CH_2Cl_2 caused immediate change of colour

from yellow to red. After stirring for 1 h the solvent was removed under vacuum to yield a brown powder. Extraction with a mixture of hexane/Et_2O afforded the yellow crystalline compound. (Yield, 66%.) Anal. Found: **C** 55.09; **H** 4.17. Calc. for $C_{18}H_{16}O_2MoS$: **C** 55.11; **H** 4.11%. Selected **IR** (KBr, cm^{-1}): 1935, 1845, vs, ν(CO). ^{1}**H** NMR ($CHCl_3$-d_1, 300 MHz, r.t., δ ppm): 7.38–7.15 (m, 5*H*, Ph); 5.29 (s, 5H, Cp); 4.30 (t, 1H); 3.85 (t, 1H); 3.76 (q, 1H); 3.53–3.50 (dd, 1H, H^6); 2.23–2.02 (m, 2H, $H^{4/5}$).

7.19. Preparation of $IndMo(\eta^3\text{-}C_5H_6SPh)(CO)_2$ (22)

Addition of excess NaPhS (0.05 g, 0.38 mmol) to a solution of $[IndMo(\eta^4\text{-}C_5H_6)(CO)_2]BF_4$ (0.07 g, 0.17 mmol) in CH_2Cl_2 caused immediate change of colour from yellow to red. After stirring for 1 h the unreacted NaPhS was filtered off and the solvent removed under vacuum to yield an oil. Very effective extraction of the residue with hexane afforded a rose-brown powder. Crystals were obtained in 60% yield by layering hexane onto a saturated solution of Et_2O. Anal. Found: **C** 59.79; **H** 3.89. Calc. for $C_{22}H_{18}O_2SMo$: **C** 59.73; **H** 4.10%. Selected **IR** (KBr, cm^{-1}): 1960; 1935; 1885; 1861, vs, ν(CO). ^{1}**H** NMR ($CHCl_3$-d_1, 300 MHz, r.t., δ ppm): 7.21–6.99 (m, 5*H*, Ph); 6.57–6.54 (m, 2H, H_{5-8}); 6.40–6.37 (m, 2H, H_{5-8}); 5.54 (t, 1H, H_2); 5.08 (d, 2H, $H_{1/3}$); 3.52 (t, 1H, H^2); 3.43 (br, 2H, $H^{1/3}$); 3.22 (dd, 1H, H^6); 1.93–1.76 (m, 1H, $H^{4/5}$).

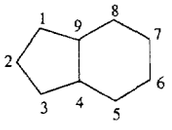

7.20. Preparation of $[CpMo(\eta^3\text{-}C_5H_6PMe_3)(CO)_2]BF_4$ (23)

Addition of excess PMe_3 (0.25 ml) to a solution of $[CpMo(\eta^4\text{-}C_5H_6)(CO)_2]BF_4$ (0.26 g, 0.70 mmol) in CH_2Cl_2 (20 ml) caused immediate precipitation of a yellow solid. After stirring for 30 min the precipitate was filtered off, washed with Et_2O and dried. The product was recrystallized from acetone/Et_2O. (Yield, 80%.) Anal. Found: **C** 40.37; **H** 4.38. Calc. for $C_{15}H_{20}O_2MoPBF_4$: **C** 40.39; **H** 4.52%. Selected **IR** (KBr, cm^{-1}): 1937; 1858, vs, ν(CO). ^{1}**H** NMR (CH_3CN-d_3, 300 MHz, r.t., δ ppm): 5.44 (s, 5H, Cp); 4.51 (t, 1H); 3.83 (m, 1H); 3.62 (m, 1H); 2.39 (m, 1H); 2.24–2.18 (m, 1H); 1.91–1.80 (m, 1H); 1.72 (d, 9H, PMe_3).

7.21. Preparation of $[CpMo(\eta^3\text{-}C_6H_8PMe_3)(CO)_2]BF_4$ (24)

Addition of PMe_3 (1 ml, excess) to a solution of $[CpMo(\eta^4\text{-}C_6H_8)(CO)_2]BF_4$ (0.49 g, 1.27 mmol) in CH_2Cl_2 caused immediate precipitation of a yellow solid. After stirring for 6 h the precipitate was filtered off, washed with Et_2O and dried. Yellow crystals in 60% yield were obtained by layering hexane onto a saturated solution of dichloromethane. Anal. Found: **C** 42.04; **H** 4.89. Calc. for $C_{14}H_{16}BF_4O_2PMo$: **C** 41.77; **H** 4.82% Selected **IR** (KBr, cm^{-1}): 1935; 1840, vs, ν(CO). ^{1}**H** NMR (CH_3CN-d_3, 300 MHz, r.t., δ ppm): 5.45 (s, 5H, Cp); 4.54 (t, 1H); 3.87 (m, 1H); 3.53 (m, 1H); 2.46 (m, 1H); 1.81 (d, 9H, PMe_3); 1.72 (m, 2H); 1.29 (m, 1H); 0.84–0.68 (m, 1H).

7.22. Preparation of $[CpMo(\eta^4\text{-}C_6H_8)(NCMe)_2]BF_4$ (25)

A solution of $[CpMo(\eta^4\text{-}C_6H_8)(CO)_2]BF_4$ (0.20 g, 0.52 mmol) in 20 ml of acetonitrile was treated with Me_3NO (0.08 g). After stirring for 2 h the solution turned red and was filtered. The solvent was evaporated and the residue washed with toluene and ether. Upon concentration and cooling the NCMe extract red crystals separated. (Yield, 80%.) Anal. Found: **C** 43.90; **H** 4.70; **N** 6.92. Calc. for $C_{15}H_{19}BF_4N_2Mo$: **C** 43.94; **H** 4.67; **N** 6.83%. Selected **IR** (KBr, cm^{-1}): ν 3115, 3053, 2998, 2980, 2936, 2275, 1058. ^{1}**H** NMR (CH_3CN-d_3, 90MHz, r.t., δ ppm): 6.18 (c, 2H, $H^{2/3}$); 4.90 (s, 5H, Cp); 3.57 (c, 2H, $H^{1/4}$); 2.27 (s, 6H, NCMe); 1.09 (c, 4H, H^{5-8}).

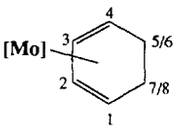

7.23. Preparation of $[CpCp'ML_2]^{2+}$ (Cp' = Cp, Ind)

Gaseous Cl_2 was bubbled (or excess of Br_2 was added) through a solution of $[Cp'Mo(\eta^4\text{-}C_5H_6)L_2]^+$ (Cp' = Cp, Ind; $L_2 = (CO)_2$, dppe) (0.70 mmol) in dichloromethane. The precipitate was filtered off and washed with CH_2Cl_2 and Et_2O. Yield > 90%. IR (KBr) and ^{1}H NMR data are in agreement with Refs. [16–18].

7.24. Reaction of $[CpMo(\eta^4\text{-}C_5H_6)(dppe)]PF_6$ with $[NBu_4]Br_3$

Addition of a solution of $[NBu_4]Br_3$ (0.08 g, 0.20 mmol) in CH_2Cl_2 to a solution of $[CpMo(\eta^4\text{-}C_5H_6)(dppe)]PF_6$ (0.15 g, 0.20 mmol) in CH_2Cl_2 caused immediate precipitation of a yellow solid. After stirring for 2 h the precipitate was filtered off, washed with Et_2O and dried. The powder thus obtained was dissolved in water and an aqueous solution of NH_4PF_6 added dropwise until no further precipitation was ob-

served. The fine precipitate was filtered off and washed with water. Recrystallization from acetone/Et_2O gave $[Cp_2Mo(dppe)][PF_6]_2$ (in 89% yield) by comparison of its IR and ^1HNMR spectra with those of an authentic sample [14].

7.25. Reaction of $[CpMo(\eta^4\text{-}C_5H_6)(dppe)]PF_6$ with $[Fc]PF_6$

A solution of $[CpMo(\eta^4\text{-}C_5H_6)(dppe)]PF_6$ (0.10 g, 0.14 mmol) in NCMe was treated with a solution of $FcPF_6$ (0.04 g, 0.13 mmol) in NCMe and refluxed for 2 h. The resulting orange solution was evaporated to dryness. The residue was washed with toluene and Et_2O until the washings were colourless. Washing with CH_2Cl_2 afforded a yellow solution from which, upon concentration and cooling, separated crystals of unreacted $[CpMo(\eta^4\text{-}C_5H_6)(dppe)]PF_6$, identified by its ^1HNMR spectrum. The residue was washed with Et_2O (2×5 ml) and recrystallized from acetone/Et_2O giving $[Cp_2Mo(dppe)][PF_6]_2$ in 45% yield.

7.26. Preparation of $[CpMo(dppe)_2][BF_4]_2$

Ph_3CBF_4 (0.08 g, 0.28 mmol) was added to a solution of $CpMo(\eta^3\text{-}C_5H_7)(dppe)$ (0.15 g, 0.24 mmol) in CH_2Cl_2. After 14 h stirring the mixture was evaporated, and the residue was washed with Et_2O, toluene and again with Et_2O. Addition of CH_2Cl_2 afforded a red solution which was filtered and evaporated to dryness. The oily residue was washed with Et_2O and $[CpMo(dppe)_2][BF_4]_2$ was isolated as a red powder in 60% yield. The remaining residue, insoluble in CH_2Cl_2, was recrystallized from acetone/Et_2O giving the dication $[Cp_2Mo(dppe)][BF_4]_2$ in 30% yield. Anal. Found: **C**, 57.29; **H**, 4.58. Calc. for $C_{37}H_{36}B_2Cl_2MoP_2$: **C**, 57.27; **H**, 4.56%. IR (KBr, cm^{-1}): ν 3060; 1600; 1480; 1435; 1430; 750; 700. **EPR spectrum**: quintet of sextets attributed to 4P equivalent and 5H. $a_{iso}P = 21.4$ G; $a_{iso}H = 2.3$ G; $g = 1.9943$. The reaction proceeds in the same way in THF.

8. Data collection

Diffraction measurements of compounds **9** and **10** were made on an Enraf-Nonius CAD4 diffractometer and for compounds **24** and **25** were made on an Enraf-Nonius TURBOCAD4 diffractometer. Data were corrected for absorption, Lorentz and polarisation effects with the CAD4 software. Other crystal data and refinement details are listed in Table 4.

9. Structure determination and refinement

In the four compounds the heavy atom positions were located in Patterson maps and the remaining non-hydrogen positions from subsequent difference Fourier maps. In **9**, **10**, **24**, and **25** complexes all the non-hydrogen atoms were refined anisotropically exception made for the C and Cl atoms of the solvent molecule of

Table 4
Crystal data and details of the structure determination of complexes **9**, **10**, **24**, **25**

	9	**10**	**24**	**25**
Formula	$C_{37}H_{35}Cl_2F_6MoP_3$	$C_{36}H_{36}MoP_2$	$C_{16}H_{22}BF_4MoO_2P$	$C_{15}H_{19}BF_4MoN_2$
Mol. wt.	853.40	626.53	460.06	410.07
Crystal system	monoclinic	monoclinic	monoclinic	monoclinic
Space group	$P2_1/c$	$P2_1/n$	$P2_1/c$	$P2_1/c$
a (Å)	10.009(1)	15.161(2)	14.853(4)	11.697(2)
b (Å)	16.119(2)	11.219(7)	6.7803(5)	7.700(7)
c (Å)	22.859(4)	17.454(3)	19.119(5)	18.442(3)
β (deg)	94.69(1)	91.02(1)	101.40(1)	98.520(1)
V (Å^3)	3675.6(9)	2968(2)	1887.4(7)	1643(2)
Z; D_{calc} (g cm^{-3})	4; 1.542	4; 1.402	4; 1.619	4; 1.658
$F(000)$	1728	1296	928	824
θ range	1.55 to 27.95	1.76 to 24.92	2.17 to 25.00	1.94 to 29.93
Index ranges	$0 \le h \le 13$, $0 \le k \le 21$, $-30 \le l \le 30$	$-17 \le h \le 17$, $0 \le k \le 13$, $0 \le l \le 20$	$-17 \le h \le 17$, $-8 \le k \le 0$, $0 \le l \le 22$	$-16 \le h \le 16$, $0 \le k \le 10$, $0 \le l \le 25$
μ (cm^{-1})	6.90	5.74	8.23	8.37
Number of collected reflections	9306	5367	3421	4137
Number of unique reflections	8815	5183	3315	4003
Number of reflections with $I \ge 2\sigma(I)$	6803	4031	2914	3434
Number of refined parameters	427	352	218	208
Final R, R_w	0.0753, 0.1957	0.0415	0.0705, 0.1648	0.0621, 0.1442
GOF	0.996	0.0788	1.068	1.057
Min/max diff. map (e Å^{-3})	1.633, −0.780	0.402, −0.734	0.898, −0.796	0.702, −1.931

complex **9**, and for the B and F atoms of the anion of the complex **24**, that were refined isotropically. The anion BF_4 of the complex **24** was found to be disordered over two different positions with occupancies of 0.53(1) and 0.47(1).

The hydrogen atoms were included in all the complexes in calculated positions and allowed to refine with group U_{iso} parameters for each of the rings and for each of the methyl groups.

Table 5
Atomic coordinates ($\times 10^4$) and equivalent isotropic displacement parameters ($Å^2 \times 10^3$) for **9**; U(eq) is defined as one third of the trace of the orthogonalized U_{ij} tensor

	x	y	z	U(eq)
Mo(1)	2190(1)	2296(1)	1498(1)	42(1)
P(1)	53(2)	2705(2)	957(1)	46(1)
P(2)	1576(2)	1017(1)	936(1)	50(1)
C(111)	−1064(8)	3475(5)	1233(4)	47(2)
C(112)	−2413(10)	3512(7)	1049(5)	75(3)
C(113)	−3224(11)	4124(7)	1240(6)	82(4)
C(114)	−2695(12)	4715(8)	1631(5)	80(3)
C(115)	−1391(12)	4688(7)	1812(4)	74(3)
C(116)	−551(10)	4085(6)	1624(4)	60(2)
C(121)	62(9)	3101(7)	205(4)	52(2)
C(122)	−644(13)	2713(8)	−263(5)	90(4)
C(123)	−591(15)	3058(9)	−826(6)	105(5)
C(124)	55(16)	3787(9)	−906(5)	105(5)
C(125)	731(12)	4159(7)	−456(5)	82(3)
C(126)	717(10)	3829(6)	105(5)	63(3)
C(131)	−986(8)	1756(5)	898(4)	52(2)
C(231)	−240(9)	1022(6)	663(5)	60(3)
C(211)	2356(9)	793(7)	244(4)	59(3)
C(212)	2173(11)	1386(8)	−210(4)	74(3)
C(213)	2628(13)	1253(10)	−738(5)	95(4)
C(214)	3302(14)	490(13)	−836(7)	121(7)
C(215)	3462(11)	−101(9)	−409(6)	81(4)
C(216)	2977(10)	68(8)	125(6)	82(4)
C(221)	1848(9)	28(5)	1332(4)	55(2)
C(222)	845(11)	−526(6)	1441(5)	73(3)
C(223)	1182(14)	−1254(6)	1735(6)	91(4)
C(224)	2455(15)	−1422(7)	1948(5)	85(4)
C(225)	3465(13)	−883(7)	1850(5)	81(3)
C(226)	3145(10)	−147(6)	1545(5)	68(3)
C(21)	701(10)	2340(6)	2232(4)	56(2)
C(22)	1757(10)	2799(7)	2442(4)	64(3)
C(23)	2829(11)	2233(6)	2730(4)	67(3)
C(24)	2509(10)	1524(6)	2341(4)	56(2)
C(25)	1135(10)	1525(6)	2163(4)	54(2)
C(11)	3934(9)	3230(5)	1727(4)	57(2)
C(12)	3208(8)	3466(6)	1200(4)	57(2)
C(13)	3359(9)	2837(6)	778(5)	62(3)
C(14)	4178(8)	2201(6)	1070(5)	60(3)
C(15)	4521(9)	2465(6)	1649(5)	60(3)
P(3)	2874(3)	5646(2)	2470(1)	69(1)
F(1)	3317(13)	5948(6)	3093(4)	177(5)
F(2)	2492(11)	5300(7)	1848(4)	161(4)
F(3)	4097(12)	6028(12)	2255(5)	273(9)
F(4)	3426(15)	4782(7)	2627(5)	200(6)
F(5)	1648(10)	5251(9)	2739(6)	211(6)
F(6)	2155(17)	6439(7)	2326(7)	248(7)
Cl(1)	4308(10)	7524(6)	593(4)	266(4)
Cl(2)	4273(16)	5748(10)	435(7)	419(8)
C(1)	5416(30)	6411(19)	742(13)	211(12)

Table 6
Atomic coordinates ($\times 10^4$) and equivalent isotropic displacement parameters ($Å^2 \times 10^3$) for **10**; U(eq) is defined as one third of the trace of the orthogonalized U_{ij} tensor

	x	y	z	U(eq)
Mo(1)	767(1)	1150(1)	2200(1)	32(1)
P(1)	743(1)	898(1)	3577(1)	34(1)
P(2)	−421(1)	−317(1)	2339(1)	34(1)
C(131)	255(4)	−543(5)	3841(4)	40(2)
C(231)	−571(4)	−767(5)	3357(3)	42(2)
C(111)	1741(4)	918(6)	4197(4)	39(2)
C(112)	2349(4)	1831(6)	4106(4)	45(2)
C(113)	3080(4)	1913(6)	4580(4)	55(2)
C(114)	3225(4)	1086(7)	5140(4)	57(2)
C(115)	2633(4)	170(7)	5239(4)	57(2)
C(116)	1889(4)	84(6)	4764(4)	45(2)
C(121)	35(4)	1946(5)	4098(4)	35(2)
C(122)	315(4)	2603(6)	4735(4)	49(2)
C(123)	−258(6)	3396(6)	5088(4)	68(2)
C(124)	−1103(5)	3532(6)	4817(5)	66(2)
C(125)	−1392(5)	2900(6)	4199(5)	60(2)
C(126)	−830(4)	2133(6)	3838(4)	50(2)
C(211)	−1584(4)	74(5)	2068(4)	40(2)
C(212)	−1744(4)	719(6)	1410(4)	61(2)
C(213)	−2584(5)	1089(7)	1198(5)	71(2)
C(214)	−3277(5)	838(7)	1674(5)	72(3)
C(215)	−3124(4)	141(8)	2311(5)	76(3)
C(216)	−2297(4)	−220(7)	2515(4)	57(2)
C(221)	−324(4)	−1801(5)	1898(4)	35(2)
C(222)	−690(4)	−2039(6)	1172(4)	50(2)
C(223)	−561(5)	−3140(7)	826(4)	57(2)
C(224)	−78(5)	−4006(7)	1191(5)	65(2)
C(225)	288(4)	−3780(6)	1889(5)	59(2)
C(226)	165(4)	−2690(5)	2243(4)	46(2)
C(11)	1076(4)	2620(6)	1328(4)	48(2)
C(12)	1264(5)	3107(6)	2045(5)	53(2)
C(13)	471(6)	3178(6)	2432(5)	56(2)
C(14)	−201(5)	2730(5)	1973(5)	49(2)
C(15)	171(4)	2368(6)	1275(4)	47(2)
C(21)	2203(4)	548(5)	2321(4)	41(2)
C(22)	1607(4)	−426(6)	2182(4)	41(2)
C(23)	1322(4)	−252(6)	1402(4)	46(2)
C(24)	2096(4)	257(6)	966(4)	54(2)
C(25)	2682(4)	839(6)	1595(4)	48(2)

Final atomic coordinates are given in Tables 5–8. Anisotropic displacement parameters for all non-hydrogen atoms, atomic coordinates and isotropic displacement parameters for all hydrogen atoms and lists of the observed and calculated structure factors, as well as complete tables of bond lengths and bond angles have been deposited as supplementary material.

All calculations required to solve and refines the structures were made using programs SHELX86 [47] and SHELX93 [48]. Drawings were made with ORTEPII [49]. The intramolecular contacts were calculated with the program PLATON [50].

10. Molecular orbital calculations

All the molecular orbital calculations were done using the extended Hückel method [38,39] with the modified H_{ij} [51]. The basis set for the metal atom consisted of ns, np, and $(n-1)$d orbitals. Only s and p orbitals were used for phosphorus. The s and p orbitals were described by single Slater-type wave functions, and the d orbitals were taken as contracted linear combinations of two Slater-type wave functions. Standard parameters were used for H, C, O, and P, while those for Mo were the following (H_{ii}/eV, ζ): 5s, −8.77, 1.96; 5p, −5.60, 1.90; 4d, −11.06, 4.452, 1.901 (ζ_2), 0.5899 (C_1), 0.5899 (C_2).

Calculations were carried out on model compounds $[Cp_2MoL_2]^{2+}$ (L = PH_3, PMe_3, PF_3, CO) and $[CpMo(\eta^4\text{-}C_5H_6)L_2]^+$ (L = PH_3, PMe_3, PPh_2H, CO), built according to the experimental structures described and mentioned in this work. The distances (Å) were, respectively Mo–Cp 2.00, C–C 1.40, C–H(sp^2) 1.08, C–H(sp^3) 1.09, Mo–P 2.44, P–H 1.42, P–C 1.80, Mo–C 1.97, C–O 1.13, and the angles (°) Cp–Mo–Cp 132.0, P–Mo–P 80.0, C–Mo–C 80.0.

No attempts at optimizing structures were made. When studying the rotation of the η^4-C_5H_6 ligand, the rest of the molecule was kept fixed, suggesting that all barriers to rotation are probably lower, though the trend should remain the same.

Table 7
Atomic coordinates (×10⁴) and equivalent isotropic displacement parameters (Å² ×10³) for **24**; U(eq) is defined as one third of the trace of the orthogonalized U_{ij} tensor

	x	y	z	U(eq)
Mo(1)	4504(1)	1486(1)	1372(1)	47(1)
P(1)	6095(2)	1751(4)	3897(1)	47(1)
C(1)	5667(6)	164(16)	1474(4)	52(2)
O(1)	6375(5)	−595(12)	1535(4)	69(2)
C(2)	5171(8)	3581(18)	1007(5)	65(3)
O(2)	5586(6)	4774(13)	773(4)	91(3)
C(11)	2900(8)	1549(29)	957(8)	99(5)
C(12)	3113(9)	−270(32)	1246(7)	103(5)
C(13)	3679(9)	−1238(21)	883(7)	91(4)
C(14)	3810(8)	−7(28)	343(6)	95(5)
C(15)	3309(9)	1675(27)	384(7)	103(5)
C(21)	5989(6)	1627(13)	2929(4)	43(2)
C(22)	5023(6)	995(13)	2607(4)	42(2)
C(23)	4336(7)	2451(17)	2438(4)	58(3)
C(24)	4607(9)	4204(17)	2165(5)	76(4)
C(25)	5531(11)	5043(17)	2441(6)	93(4)
C(26)	6289(9)	3521(17)	2631(5)	75(3)
C(111)	5811(7)	−547(16)	4232(5)	62(3)
C(112)	5334(10)	3540(19)	4146(5)	95(5)
C(113)	7255(8)	2305(21)	4313(6)	88(4)
B(1)	8242(10)	7380(24)	3628(8)	72(3)
F(1)	8795(10)	8253(24)	4152(8)	93(5)
F(2)	7402(10)	7107(22)	3800(8)	71(4)
F(3)	8536(11)	5331(27)	3666(10)	97(6)
F(4)	8675(20)	7954(53)	3101(16)	173(11)
F(11)	8261(21)	9359(52)	3432(17)	196(13)
F(12)	8345(17)	6441(42)	3047(14)	165(9)
F(13)	7346(13)	7650(31)	3472(11)	115(6)
F(14)	8654(22)	6457(55)	4193(20)	221(14)

Table 8
Atomic coordinates (×10⁴) and equivalent isotropic displacement parameters (Å² ×10³) for **25**; U(eq) is defined as one third of the trace of the orthogonalized U_{ij} tensor

	x	y	z	U(eq)
Mo(1)	4050(1)	1145(1)	1496(1)	30(1)
N(1)	4433(5)	1744(7)	2641(3)	40(1)
C(11)	4618(6)	1908(10)	3262(4)	44(2)
C(12)	4879(8)	2074(12)	4053(4)	65(2)
N(2)	5716(5)	−88(7)	1729(3)	43(1)
C(21)	6523(7)	−897(9)	1863(4)	47(2)
C(22)	7549(7)	−1955(12)	2041(5)	66(2)
C(111)	2855(8)	3985(10)	394(4)	67(3)
C(112)	3275(7)	3872(8)	1207(4)	50(2)
C(113)	4464(7)	4072(8)	1458(4)	51(2)
C(114)	5188(7)	3182(10)	1063(5)	56(2)
C(115)	4654(8)	2178(9)	464(4)	54(2)
C(116)	3658(9)	3010(11)	−32(4)	69(3)
C(211)	3322(7)	−1323(9)	1856(4)	54(2)
C(212)	3546(7)	−1598(9)	1133(4)	52(2)
C(213)	2821(8)	−539(11)	672(4)	59(2)
C(214)	2145(7)	431(10)	1088(5)	65(3)
C(215)	2445(7)	−46(12)	1831(5)	62(2)
B(1)	6003(10)	−2729(15)	3724(6)	63(3)
F(1)	6689(7)	−1373(12)	3634(5)	136(3)
F(2)	5488(7)	−3350(11)	3068(4)	128(3)
F(3)	6587(13)	−3985(13)	4039(5)	241(7)
F(4)	5248(9)	−2221(15)	4134(7)	207(6)

Acknowledgements

This work was financially supported by JNICT under project PMCT/C/CEN/659/90 and PRAXIS XXI under project 2/2.1/QUI/316/94. ISG, CAG and JPL thank PRAXIS XXI for a grant. The authors thank the group of Professor M.H. Garcia (University of Lisbon) for providing the facilities and help necessary for the electrochemical studies.

References

[1] J.W. Faller, H.H. Murray, D.L. White, K.H. Chao, Organometallics 2 (1983) 400.
[2] A.J. Pearson, Md.N.I. Khan, Tetrahedron Lett. 25 (1984) 3507.
[3] A.J. Pearson, Md.N.I. Khan, J.C. Clardy, H. Cun-heng, J. Am. Chem. Soc. 107 (1985) 2748.
[4] M. Green, S. Greenfield, M. Kersting, J. Chem. Soc. Chem. Commun. (1985) 18.
[5] M. Bottril, M. Green, J. Chem. Soc. Dalton Trans. (1977) 2635.
[6] A.J. Pearson, Md.N.I. Khan, J. Org. Chem. 50 (1985) 5276.
[7] S.G. Davies, M.L.H. Green, D.M. Mingos, Nouv. J. Chim. 1 (1977) 445.
[8] S.G. Davies, M.L.H. Green, D.M. Mingos, Tetrahedron 34 (1978) 3047.

[9] L.A.P. Kane-Maguire, E.D. Honig, D.A. Sweigart, Chem. Rev. 84 (1984) 525.
[10] T. Hudliky, J.D. Price, Chem. Rev. 89 (1989) 1467.
[11] B.E. Bursten, M.R. Callstrom, C.A. Jolly, L.A. Paquette, M.R. Sivik, R.S. Tucker, C.A. Wartchow, Organometallics 13 (1994) 127.
[12] D.W. Macomber, W.P. Hart, M.D. Rausch, Adv. Organomet. Chem. 21 (1982) 1.
[13] C. Janiak, H. Schumann, Adv. Organomet. Chem. 33 (1991) 291.
[14] T. Aviles, M.L.H. Green, A.R. Dias, C.C. Romão, J. Chem. Soc. Dalton Trans. (1979) 1367.
[15] a) H. Brunner, R. Lukas, J. Organomet. Chem. 90 (1975) C25; b) R.R. Rodgers, W.E. Hunter, J.L. Atwood, J. Chem. Soc. Dalton Trans. (1980) 1032.
[16] J.R. Ascenso, C.G. de Azevedo, I.S. Gonçalves, E. Herdtweck, D. Moreno, C.C. Romão, J. Zühlke, Organometallics 13 (1994) 429.
[17] I.S. Gonçalves, C.C. Romão, J. Organomet. Chem. 486 (1995) 155.
[18] J.R. Ascenso, C.G. de Azevedo, I.S. Gonçalves, E. Herdtweck, D.S. Moreno, M. Pessanha, C.C. Romão, Organometallics 14 (1995) 3901.
[19] B.S. McGilligan, T.C. Wright, G. Wilkinson, M. Motevalli, M.B. Hursthouse, J. Chem. Soc. Dalton Trans. (1988) 1737.
[20] E. Gore, M.L.H. Green, J. Chem. Soc. (A) (1970) 2315.
[21] J.R. Ascenso, M.D. Carvalho, A.R. Dias, C.C. Romão, M.J. Calhorda, L.F. Veiros, J. Organomet. Chem. 470 (1994) 147.
[22] C.G. de Azevedo, A.R. Dias, A.M. Martins, C.C. Romão, J. Organomet. Chem. 368 (1989) 57.
[23] a) S.G. Davies, S.D. Moon, S.J. Simpson, S.E. Thomas, J. Chem. Soc. Dalton Trans. (1983) 1805; b) H.E. Bunting, M.L.H. Green, P.A. Newman, J. Chem. Soc. Dalton Trans. (1988) 557.
[24] M.J. Calhorda, M.G.B. Drew, V. Félix, I.S. Gonçalves, C.C. Romão, (submitted).
[25] B.R. Francis, M.L.H. Green, T. Luong-thi, G.A. Moser, J. Chem. Soc. Dalton Trans. (1976) 1339.
[26] M.L.H. Green, W.E. Lindsell, J. Chem. Soc. (A) (1967) 1455.
[27] J.A. Segal, M.L.H. Green, J.-C. Daran, K. Prout, J. Chem. Soc. Chem. Commun. (1976) 766.
[28] K. Prout, J.-C. Daran, Acta. Cryst. B 33 (1977) 2303.
[29] J.M. Almeida, I.S. Gonçalves, C.C. Romão, Anales de Química Int. Ed. 93 (1997) 8.
[30] M.L.H. Green, J. Knight, J.A. Segal, J. Chem. Soc. Dalton Trans. (1977) 2189.
[31] E. Cannillo, K. Prout, Acta Cryst. B 33 (1977) 3916.
[32] J.W. Faller, D.F. Chodosh, D. Katahira, J. Organomet. Chem. 187 (1980) 227.
[33] J.W. Faller, K.H. Chao, H.H. Murray, Organometallics 3 (1984) 1231.
[34] J.W. Faller, Y. Shvo, K. Chao, H.H. Murray, J. Organomet. Chem. 226 (1982) 251.
[35] M. Green, S. Greenfield, J. Grimshire, M. Kersting, A.G. Orpen, R.A. Rodrigues, J. Chem. Soc. Chem. Commun. (1987) 97.
[36] A.J. Pearson, S. Mallik, R. Mortezai, M.W.D. Perry, R.J. Shively Jr., W.J. Youngs, J. Am. Chem. Soc. 112 (1990) 8034.
[37] F.H. Allen, J.E. Davies, J.J. Galloy, O. Johnson, O. Kennard, C.F. Macrae, D.G. Watson, J. Chem. Inf. Comput. Sci. 31 (1991) 204.
[38] R. Hoffmann, J. Chem. Phys. 39 (1963) 1397.
[39] R. Hoffmann, W.N. Lipscomb, J. Chem. Phys. 36 (1962) 2179, 3489.
[40] A.R. Dias, C.C. Romão, J. Organomet. Chem. 233 (1982) 223.
[41] a) J.P. McNally, D. Glueck, N.J. Cooper, J. Am. Chem. Soc. 110 (1988) 4838; b) J.P. McNally, N.J. Cooper, J. Am. Chem. Soc. 111 (1989) 4500; c) T.C. Forschner, N.J. Cooper, J. Am. Chem. Soc. 111 (1989) 7420.
[42] M.L. Luetkens Jr., A.P. Sattelberger, H.H. Murray, J.D. Basil, J.P. Fackler Jr., Inorg. Synth. 28 (1990) 305.
[43] a) A.P. Pearson, Aust. J. Chem. 30 (1977) 345; b) A.P. Pearson, Aust. J. Chem. 29 (1976) 1101.
[44] E.M. Kaiser, C.R. Hauser, J. Org. Chem. 33 (1968) 3402.
[45] I.V. Nelson, R.T. Iwamoto, Anal. Chem. 35 (1963) 867.
[46] H. Schmidbauer, H. Stuhler, W. Vornberger, Chem. Ber. 105 (1972) 1084.
[47] G.M. Sheldrick, in: G.M. Sheldrick, C. Krüger, R. Goddard (Eds.), SHELX-86, Crystallographic Computing 3, Oxford University Press, 1985, p. 175.
[48] G.M. Sheldrick, SHELX-93, A Computer Program for Crystal Structure Determination, University of Göttingen, Germany, 1993.
[49] C.K. Jonhson, ORTEP-II, A Fortran Thermal-ellipsoid Plot Program for Crystal Structure Illustrations, Report ORNL-5318, Oak Ridge National Laboratory, TN, 1976.
[50] A.L. Spek, PLATON, Acta Cryst. A 46 (1990) C31.
[51] J.H. Ammeter, H.-B. Bürgi, J.C. Thibeault, R. Hoffmann, J. Am. Chem. Soc. 100 (1978) 3686.